HAL open science

Geometric Optimal Control of the Generalized Lotka-Volterra Model of the Intestinal Microbiome

Bernard Bonnard, Jérémy Rouot, Cristiana Silva

To cite this version:

Bernard Bonnard, Jérémy Rouot, Cristiana Silva. Geometric Optimal Control of the Generalized Lotka-Volterra Model of the Intestinal Microbiome. Optimal Control Applications and Methods, 2024, 10.1002/oca.3089 . hal-03861565v2

HAL Id: hal-03861565

https://hal.science/hal-03861565v2

Submitted on 6 Feb 2024

HAL is a multi-disciplinary open access archive for the deposit and dissemination of scientific research documents, whether they are published or not. The documents may come from teaching and research institutions in France or abroad, or from public or private research centers.

L'archive ouverte pluridisciplinaire **HAL**, est destinée au dépôt et à la diffusion de documents scientifiques de niveau recherche, publiés ou non, émanant des établissements d'enseignement et de recherche français ou étrangers, des laboratoires publics ou privés.

Received: Added at production | Revised: Added at production | Accepted: Added at production

DOI: xxx/xxxx

ARTICLE TYPE

Geometric Optimal Control of the Generalized Lotka–Volterra Model of the Intestinal Microbiome

Bernard Bonnard[1,2] | Jérémy Rouot[3] | Cristiana Silva[4,5]

[1]Université de Bourgogne Franche-Comté, Institut de Mathématiques de Bourgogne, Dijon, France
[2]Inria Sophia Antipolis, Sophia Antipolis, France
[3]Univ Brest, UMR CNRS 6205, Laboratoire de Mathematiques de Bretagne Atlantique, Brest, France
[4] Iscte - Instituto Universitário de Lisboa, Lisbon, Portugal
[5]Center for Research and Development in Mathematics and Applications (CIDMA), Aveiro, Portugal

Correspondence
Jérémy Rouot, Univ Brest UMR CNRS 6205, Laboratoire de Mathématiques de Bretagne Atlantique. Email: jeremy.rouot@univ-brest.fr

Summary

We introduce the theoretical framework from geometric optimal control for a control system modeled by the Generalized Lotka-Volterra (GLV) equation, motivated by restoring the gut microbiota infected by Clostridium difficile combining antibiotic treatment and fecal injection. We consider both permanent control and sampled-data control related to the medical protocols.

KEYWORDS:
Optimal control in the permanent case, sampled-data control, biomathematics and population dynamics

1 | INTRODUCTION

Complex microbial communities controlled by a combination of continuous controls associated to probiotics and bacteriostatic agents and impulsive controls corresponding to transplantation and bactericides can be modeled by a generalized Lotka-Volterra (GLV) model [1].

In this frame, our study is motivated by the original works described in [12] and based on the experimental model from [24] to treat the Clostridium Difficile Infection (CDI) of the gut microbiota using the medical combination of taking antibiotics followed by a fecal injection. The system is modeled by a GLV equation with eleven interacting species and the parameters are reported in Table C1 excerpted from [12].

The originality of our study is to set the problem in a neat geometric optimal control framework to use the techniques of this area, see for instance [13, 26] as a general references to be applied to the specific controlled equation and the objective being to minimize the C. difficile population.

The GLV equation is interpreted as a model of interaction of different equilibria where the optimal problem is analyzed with geometric optimal control techniques based on (intrinsic) Lie algebraic computations to derive robust control schemes in the permanent case. It is completed by sampled-data optimal control techniques, taking into account digital restrictions on the controls related to medical constraints.

[0]**Abbreviations:** GLV, Generalized Lotka-Volterra; C. difficile: Clostridium difficile; CDI : Clostridium Difficile Infection

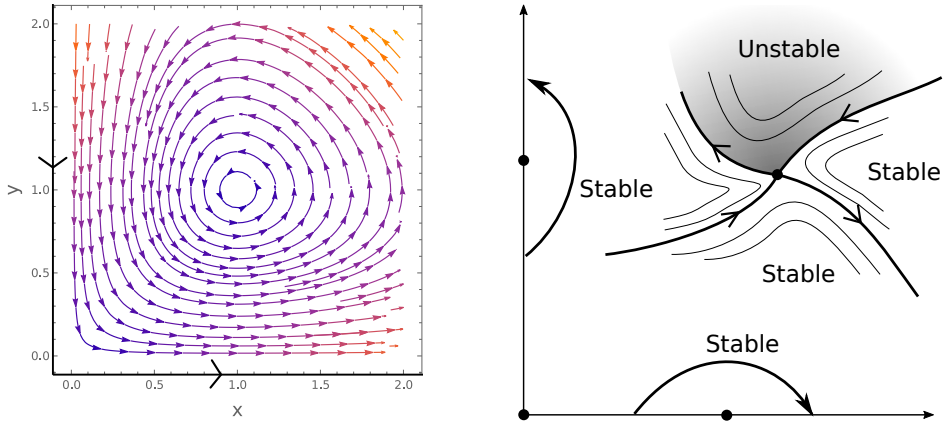

FIGURE 1 *(left) Phase portrait of* (1). *(right)* Model with 2 centers and a saddle displaying an unstable domain related to separatrices.

1.1 | A pedestrian presentation of the controlled model

The historical model of Lotka–Volterra [27, 21] starts by describing the interaction of two populations of prey-predator denoted respectively by x, y and the evolution of the two species is described by the system

$$\begin{aligned} \dot{x} &= x(\alpha - \beta y), \\ \dot{y} &= y(\delta x - \gamma), \end{aligned} \tag{1}$$

where $\alpha, \beta, \delta, \gamma$ are positive parameters and $x, y \in \mathbb{R}^+$.

Such dynamics admits two equilibrium points:

$$\theta_1 = (0, 0) \text{ and } \Omega = (\gamma/\delta, \alpha/\beta)$$

and a first integral

$$V(x, y) = \beta y + \delta x - \alpha \log y - \delta \log x.$$

Since every trajectory evolves on the level sets of V, one deduces that Ω is a center, that is every trajectory is periodic, for each initial condition in the physical quadrant. Behaviors of the solutions are represented on Fig.1 (left).

The second step in our analysis is to use the historical model to construct a $2d$–topological model to describe the evolution of the dynamics related to the interaction between two centers. This leads to construct a $2d$–model, with a schematic representation in Fig.1 (right). The important point of the construction is to introduce in the domain a saddle point with separatrices and an unstability domain.

A $2d$–realization leads to the $2d$–GLV generalization of (1):

$$\begin{aligned} \dot{x} &= x(r_1 + a_{11}x + a_{12}y) \\ \dot{y} &= y(r_2 + a_{21}x + a_{22}y), \end{aligned} \tag{2}$$

which is precisely the reduced model described in [12] to control the CDI.

Following [27] this leads to introduce the GLV-model whose aim is to describe using a quadratic dynamics, interaction between equilibria in arbitrary dimension. We proceed as follows.

Let $x = (x_1, x_2, \dots, x_N) \in \mathbb{R}_+^N$, the dynamics is

$$\dot{x} = (\operatorname{diag} x)\,(Ax + r)\,, \tag{3}$$

where A is the interaction matrix.

In the regular case it can admit up to 2^N equilibria, which can be easily computed recursively using the rule:

- Interior equilibrium: $x = -A^{-1}r$, which is called persistent.
- Boundary equilibrium: $x_i = 0$ and we obtain a system with the same representation as (3) of size $N - 1$ and we compute the equilibria by induction.

Stein et al. model [24] describes the C. difficile infection with $N = 11$ and the variable x_1 represents the C. difficile population. Control schemes can be introduced in the model as follows.

- *Antibiotic treatment.* We denote by $Y(x)$ the linear dynamics: $Y(x) = (\varepsilon_1 x_1, \dots, \varepsilon_N x_N)^\intercal$, where $\varepsilon_i \leq 0$, $i = 1, \dots, N$ denotes the *sensitivity* of the x_i variable to the *antibiotic*, so that the controlled dynamics takes the form:

$$\frac{\mathrm{d}x}{\mathrm{d}t}(t) = X(x(t)) + u(t)Y(x(t)), \quad u \in [0, 1], \tag{4}$$

  where $X(x) = (\operatorname{diag} x)\ (Ax + r)$ is the GLV-equation and the various parameters are identified in [24] and reported in Table C1, while $Y(x) = \operatorname{diag} x \left(\varepsilon_1, \dots, \varepsilon_N\right)^\intercal$.

  The control $u(\cdot)$ valued in [0, 1] describes the dosing regimen represented by a piecewise constant mapping.

  One can use log–coordinates: $x = e^y$ so that the dynamics takes the form

$$\dot{y} = (A\, e^y + r) + u\, \boldsymbol{\varepsilon},$$

  where $\boldsymbol{\varepsilon} = (\varepsilon_1, \dots, \varepsilon_N)^\intercal$ is a constant vector.

- *Probiotic agents.* They are associated to a linear vector field: $(\varepsilon'_1 x_1, \dots, \varepsilon'_N x_N)^\intercal$, with $\varepsilon'_i \geq 0$ versus $\varepsilon_i \leq 0$ for an antibiotic agent.

The second type of controls are impulsive controls corresponding to a Dirac at time t_1, with height λ given by $\lambda\delta(t - t_1)$ in a vector direction v. Such Dirac is the limit of piecewise constant control: $\lim_{n\to\infty} u = n$ on $[t_1, t_1 + t/n]$ of the control system:

$$\frac{\mathrm{d}x}{\mathrm{d}t}(t) = X(x(t)) + u(t)Y'(x(t)), \quad u \in \mathbb{R}$$

with $Y'(x) = v$ is constant.
Hence this leads to modify instantaneously the state variable $x \to x + \lambda v$. Such a control action can be applied at discrete times of intervention $\mathcal{T} = (t_1, t_2, \dots)$ and are invasive treatment, which can be:

- fecal injection, if $\lambda > 0$
- bactericide, if $\lambda < 0$.

In the protocol presented in [12], it consists into: antibiotic treatment starting at time $t = 0$ for an healthy mouse, followed by C. difficile infection and a single fecal injection.
This leads to analyze the control system:

$$\dot{x} = X(x) + uY(x), \quad u \in [0, 1], \tag{5}$$

where u is associated to antibiotic administration, using either:

- a *permanent control* $u(\cdot)$ taken as a measurable mapping which in practice is approximated by a piecewise constant mapping.
- or a *sampled-data control*. In this case, during the therapy period one has a fixed number of medical interventions defined by:
  - the control u is piecewise constant and defined by a fixed sequence of constant controls u_i on $[t_i, t_{i+1}]$, $t_0 = 0$, $t_i - t_{i-1} \geq I_m > 0$, $i = 1, \dots, k$.

We shall focus the minimization of the C. difficile infection, which leads to a Mayer problem

- OCP1: $\min_{u(\cdot)}\ x_1(t_f)$, t_f being the time duration of the therapy,

and a dual formulation:

- OCP2: $\min_{u(\cdot)}\ t$, with a target $x_1 = d$, d being a fixed nonnegative constant.

The above problem in the permanent and digital case can be analyzed using optimal control direct and indirect methods.
Indirect methods are based on the Maximum Principle stated for the permanent case [19, 23] or for the sampled-data control case [9].

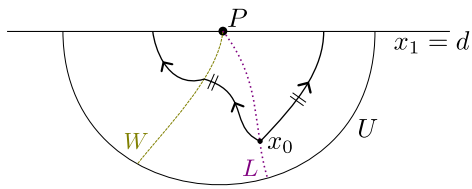

FIGURE 2 Schematic representation of the construction of the synthesis in a neighbourhood U of a point P of the terminal manifold $x_1 = d$ with a switching locus W and a cut point at x_0 belonging to the separating locus L.

1.2 | Permanent case: Maximum Principle.

We shall consider the control system

$$\dot{x} = X(x) + u\,Y(x), \quad |u| \leq 1$$

and the problem of reaching in minimum time t^* the target $\boldsymbol{N} : x_1 = d$ (with in practice some additional constraint related to stability property).

Introducing the Hamiltonian lift of the system defines the pseudo (or non maximized) Hamiltonian

$$H(z,u) = p \cdot (X(x) + u\,Y(x))$$

where $z = (q,p)$, $p \in \mathbb{R}^N \setminus \{0\}$ (adjoint vector), the Maximum Principle tells us that candidates as minimizers are solutions of the dynamics

$$\begin{aligned} \dot{x} = \frac{\partial H}{\partial p}, \quad \dot{p} = -\frac{\partial H}{\partial q}, \\ H(z,u) = \max_{v \in [0,1]} H(z,v), \end{aligned} \tag{6}$$

where p satisfies at the final time t^* the transversality condition:

$$p(t^*) \perp T_{x(t^*)}\boldsymbol{N}$$

and moreover $M(z) = \max_{v\in[0,1]} H(z,v)$ is a nonnegative constant.

The aim of geometric optimal control is to construct the time minimal synthesis: $u^*(x_0)$ for every initial condition x_0 (see Fig.2). This amounts to compute:

- the switching locus W, where the optimal control is discontinuous,
- the separating locus L, where two minimizers intersect,
- the cut locus C, where a control ceases to be minimizing.

There is a lot of results coming from a series of article [5, 17] to compute explicit semi-algebraic approximations of switching, separating and cut loci in a tubular neighborhood of $\boldsymbol{N}$ using Lie algebraic computations only, and suitable in our analysis. It will serve to construct in fine a decomposition of $\mathbb{R}^N$ into bands $d \leq x_i \leq d+\varepsilon$ to patch the different local syntheses to construct suboptimal policies to transfer the system from an infected point to an healthy point (see Fig.3). Clearly in this analysis the behaviors of the system near forced equilibria localized on the set $\mathcal{C}$, where X and Y are collinear, is crucial. This set contains the (free) equilibria of the GLV-dynamics. The key point of the model is that the collinear set can be computed using linear computations only.

1.3 | Sampled-data case.

The optimal control problem can be interpreted as a finite dimensional optimization problem and solved in this context. Adapted numerical choice is to use a MPC method, but non linearity comes from the dynamics. Convergence is related to the regularity properties of the time minimal value function analyzed using geometric optimal control analysis in the permanent case. Strong pathologies can occur in relation with accessibility properties. This will be discussed in details and this is the core of this article.

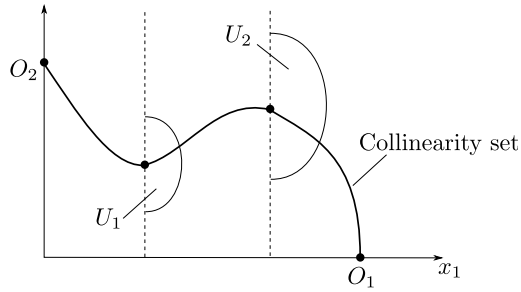

FIGURE 3 Schematic representation of a path between two open sets U_1 and U_2 on which the synthesis have been determined.

1.4 | The organization of the article

The article is organized in three sections.

In Section 2 we introduce the controlled Generalized Lotka-Volterra equation associated to the problem of reducing C. difficile infection. We present the techniques from geometric optimal control to be applied to the analysis in relation with accessibility property of the system. In this context singular trajectories are defined as singularities of the extremity mapping.

In Section 3, the optimal control problem aiming to reduce C. difficile infection is analyzed using indirect methods (maximum principles) in both permanent and non permanent cases, to derive ncessary optimality conditions. Such conditions are used in the permanent case to the geometric classification of the regular syntheses near a terminal manifold of codimension one. They can be glued together to construct global syntheses in our study.

In Section 4, the techniques are applied to the controlled Lotka–Volterra model. First we concentrate on the $2d$–case. The geometric study is showed to be related to the interaction between the collinearity and the singularity loci, which reduces in the model to two straight-lines. Numerical results are presented combining direct and model predictive control methods. Computations are extended to the $3d$–case, determining the singular trajectories and they are classified according to their time optimality status. This is applied to the May–Leonard model [22].

2 | CONTROLLED GLV-MODEL AND GEOMETRIC OPTIMAL CONTROL

2.1 | Controlled GLV-equation

2.1.1 | Definitions

The *C. difficile* infected GLV-equation is the dynamics described by:

$$\dot{x} = (\operatorname{diag} x)\ (Ax + r) = \sum_{i=1}^{N} x_i (Ax + r)_i\, e_i \tag{7}$$

with e_i is the *ith* vector of the canonical basis of $\mathbb{R}^N$, $x = \left(x_1, x_2, \dots, x_N\right) \in \mathbb{R}_+^N$, where x_1 represents the *C. difficile* population and $\tilde{x} = \left(x_2, \dots, x_N\right) \in \mathbb{R}_+^{N-1}$ describes the healthy agents. The matrix $A = \left(a_{ij}\right)$ is the matrix of interaction, where a_{ij} represents the birth or death rate of the i-agent with respect to the j-agent and r represents the birth or death rate of the i-agent without interaction. Note that the healthy agents can be ordered as $x_2 < x_3 < \dots < x_N$ according to the coefficients a_{ij}. We denote by $M^+ = \mathbb{R}_+^N$ the invariant domain $x_i > 0$, $\bar{M}^+$ the union of the M^+ with its boundary. Moreover, the dynamics (7) can be extended to the whole Euclidean set $\mathbb{R}^N$. Using log-coordinates $x = e^y$, we denote by M the log-image of M^+.

The dynamics is called *regular* if A is invertible and we denote by x_i the infected persistent equilibrium point $x_e = -A^{-1}\, r$. Making $x_1 = 0$ in (7), this defines a restricted healthy dynamics given by

$$\dot{\tilde{x}} = \tilde{x}\ \left(\tilde{A}x + \tilde{r}\right),$$

where $\tilde{x} = \left(x_2, \dots, x_N\right) \in \mathbb{R}_+^{N-1}$.

In the regular case, the dynamics can admit up to 2^N equilibria, which can be easily computed by recurrence making $x_i = 0$ in (7).

Since (7) is polynomic, asymptotic behaviors can be determined using the standard Poincaré compactification with the embedding of (7) into the hyperplane $(x, z = 1)$ of $\mathbb{R}^{N+1}$ to define:

$$\dot{x} = (\operatorname{diag} x)\,(Ax + rz)$$
$$\dot{z} = 0,$$

where the right-member has been homogeneized to define an homogeneous quadratic vector of $\mathbb{R}^{N+1}$, which can be projected on the N-sphere S^N.

Each equilibrium can be classified according to their L(linear)-stability status associated to the linearized system [18].

Our study is related to the interaction of the computable k-equilibria of the dynamics and one can construct a polynomic system denoted P_2 in a domain U centered at x_e with the k-equilibria defined by the k-interacting equilibria of the original system and preserving their L-stability. Such polynomial system leads to introduce the dynamics

$$\dot{x} = P_2(x),$$

which can be extended on the whole $\mathbb{R}^N$. Again it can be compactified and the equilibria distinct from x_e are at the infinity.

2.1.2 | Antibiotic action

In this article, we shall mainly restrict to the case of a *single antibiotic treatment* and a final fecal injection to fit to the protocol therapy described in [12]. At time $t = 0$, antibiotic treatment can be either administrated at different dosing regimens: constant dosing regimen, a pulsed dosed regimen or a tapered dosing regimens. The control system takes the form:

$$\dot{x} = X(x) + u\,Y(x)\,,$$

with $X = (\operatorname{diag} x)\,(Ax + b)$ and $Y(x) = (\operatorname{diag} x)\left(\varepsilon_1, \dots, \varepsilon_N\right)^T$, where ε_i are the *sensitivity coefficients*.

The control $u(t)$ describes the dosing regimen, a single pulse corresponds to a Dirac, with height λ as a limit when $n \to +\infty$ $u(t) = n\,\lambda$ over $\left[0, 1/n\right]$ or a constant regimen with $u(t) = m$.

This leads to consider a general control system of the form:

$$\dot{x} = X(x) + u\,Y(x)\,, \quad u \in [0, +\infty[\ .$$

Note that using *probiotics* means to reverse the antibiotics actions using $\varepsilon_i \to -\varepsilon_i$, and the parameters ε_i being related to the choice of antibiotics or probiotics.

2.1.3 | Fecal injection

In the protocol described in [12], after a preliminary administration of antibiotic to an uninfected individual, *C. difficile* is inoculated to jump to an infected state and a final single fecal injection is administrated.

Hence, this leads to consider the time minimal control problem for the single-input control system:

$$\dot{x} = X(x) + u\,Y(x)\,, \quad u \in [0, m]\,,$$

where the terminal target is the manifold $\{x_1 = d\}$. In the protocol, a constant antibiotic injection has the effect of *shifting the equilibria* of the free motion, and the final fecal injection has no effect on the x_1-population but is related to enter in a *stability domain* in the terminal manifold. Hence, one can restrict our analysis to the antibiotic treatment either in the permanent case or in the control-data frame.

2.2 | Controllability and feedback linearization

2.2.1 | Preliminaries

In this section, the system $\dot{x} = X(x) + u\,Y(x)$, $u \in [0, 1]$, is denoted by $F(x, u)$ and the control u is extended to the whole $\mathbb{R}$ and is shortly written as (X, Y). The *feedback pseudo-group* is denoted by G_f and is the set of triplets (φ, α, β), where φ is a local diffeomorphism, $u = \alpha(x) + \beta(x)v$, $\beta \neq 0$ is a feedback and acts on (X, Y) according to the action $(X, Y) \mapsto (\varphi * (X + \alpha Y)\,, \varphi * \beta Y)$.

Definition 1. Let (x, u) be a control trajectory pair defined on $[0, T]$, the linearized system along the reference pair (x, u) is the time dependent variational linear system

$$\dot{\delta x} = A(t)\delta x + B(t)\delta u \quad \text{with} \quad A(t) = \frac{\partial F}{\partial x}(x(t), u(t)), \; B(t) = \frac{\partial F}{\partial u}(x(t), u(t)) \; .$$

Next, we introduce the concept of singular trajectories with crucial properties, see [4] for more details. Recall that $E^{x_0,T}$ denotes the extremity mapping where the set $\mathcal{U}$ of controls is endowed with the $L^\infty([0, T])$ norm (see Appendix A).

Definition 2. A control trajectory pair (x, u) is singular on $[0, T]$ if the Fréchet derivative of the extremity mapping is not of maximal rank: $n = \dim\ M$.

One has the following proposition.

Proposition 1. The Fréchet derivative of the extremity mapping at (x, u) solution of the linearized system:

$$\begin{cases} \dot{\delta x}(t) = A(t)\delta x(t) + B(t)\delta v(t) \\ \delta x(0) = 0\,, \end{cases}$$

and the pair (x, u) is singular if and only if there exists a non zero adjoint vector p on $[0, T]$ such that $t \to x(t)$ is the projection of the solution of the Hamiltonian system:

$$\begin{cases} \dot{x} = \frac{\partial H_F}{\partial p}(x, p, u)\,, \quad \dot{p} = -\frac{\partial H_F}{\partial x}(x, p, u)\,, \\ \frac{\partial H_F}{\partial u} = H_Y = 0\,, \end{cases} \tag{8}$$

where $H_F := p \cdot F(x, u)$ and $H_Y = p \cdot Y(x)$ are the Hamiltonian lifts.

Proposition 2. Singular trajectories are feedback invariant that is G_f acts on the set of singular trajectories by change of coordinates only (lifting a diffeomorphism φ into a Mathieu symplectomorphism).

Definition 3. The system $F(x, u)$ is called *feedback linearizable* if for the action of the pseudo-group G_f it is equivalent to the time-invariant controllable linear system $\dot{x} = Ax + Bu$, where A, B are constant matrix.

One has the following proposition [11, p.165].

Proposition 3. The system $F(x, u) = X + uY$ is feedback linearizable near a point $x_0 \in M$ if and only if

1. the matrix $\{Y(x_0), \mathrm{ad}\, X \cdot Y(x_0), \ldots, \mathrm{ad}^{n-1} X \cdot Y(x_0)\}$ has rank $n = \dim\ M$ at x_0;
2. the distribution $D = \mathrm{span}\,\{Y, \mathrm{ad}\, X \cdot Y, \ldots, \mathrm{ad}^{n-2}\, X \cdot Y\}$ is involutive, that is, $[D, D] \subset D$ near x_0.

Clearly, the existence of singular trajectories is an obstruction to feedback linearization, see [1] for the applications to microbial communities.

Computations of singular trajectories.

One uses the system (8) computations being neat with the iterated Poisson brackets $\{H_X, H_Y\} = \mathrm{d}\vec{H}_X\left(H_Y\right) = H_{[X,Y]}$.

From (8), one has $H_Y = 0$ and deriving twice with respect to time one gets

$$\begin{aligned} &H_Y(z(t)) = \{H_Y, H_X\}(z(t)) = 0, \\ &\{\{H_Y, H_X\}, H_X\}(z(t)) + u(t)\,\{\{H_Y, H_X\}, H_Y\}(z(t)) = 0\,. \end{aligned} \tag{9}$$

The singular control denoted u_s associated to the extremal lift $t \mapsto z(t) = (x(t), p(t))$ is called of *minimal order 2* if the following regularity condition is satisfied

$$\{\{H_Y, H_X\}, H_Y\}(z) = p \cdot [[Y, X], Y](x) \neq 0\,,$$

along the extremal $t \mapsto (p(t), x(t))$.

Otherwise from (9), one gets:

$$\begin{aligned} &\{\{\{H_Y, H_X\}, H_X\}, H_X\}(z) + u\,\{\{\{H_Y, H_X\}, H_X\}, H_Y\}(z) = 0\,, \\ &\{\{\{H_Y, H_X\}, H_Y\}, H_X\}(z) + u\,\{\{\{H_Y, H_X\}, H_Y\}, H_Y\}(z) = 0\,, \end{aligned} \tag{10}$$

and if again $u(\cdot)$ can be deduced from the two previous linear equations, the corresponding control u_s is called of *order* 3. One can iterate the computation to deduce singular arcs at *any order*.

One application to controllability which generalizes the standard controllability result by linearization from [19] is the following.

Theorem 1. Let (x, u) be a control trajectory pair on $[0, T]$ and assume that (x, u) is not singular. Then the image of the extremity mapping at $u(\cdot)$ is open that is there exists an open set W, centered at $x(T) = E^{x(0),T}(u)$ such that $W \subset A^+(x_0, T)$ (provided the control u is strictly feasible).

Remark 1. The previous results can be applied to our study with some care to deal with *feasible controls*. Indeed, in practice, one has a constraint $u \in [0, 1]$. Hence, this leads to consider only controls such that u is *strictly admissible*, that is $0 < u < 1$. If $u = 0$ or $u = 1$, u is said *saturating* the control constraints.

3 | A GEOMETRIC APPROACH TO OPTIMAL CONTROL: THE PERMANENT *VERSUS* DIGITAL CASE

3.1 | Notations

In this section, we use the notation $\dot{x} = F(x) + u\,G(x)$, $|u| \leq 1$, so that, the cone C of admissible directions is generated by $F \pm G$, that is $X = F - G$, $Y = 2\,G$.

3.2 | Maximum Principle

Permanent case

First of all, we must introduce the notations and definitions related to the Maximum Principle. Consider the control system $\dot{x} = F + uG$, $|u| \leq 1$. Denote by $H = H_F + uH_G$ the Hamiltonian lift with $H_F(z) = p \cdot F(x)$, $H_G = p \cdot G(x)$, with $x \in M \simeq \mathbb{R}^N$. Let $\boldsymbol{N}$ be a terminal manifold and consider the time minimal control problem, with terminal manifold $\boldsymbol{N}$. The Maximum Principle [19] tells us that if (x, u) is a time minimal trajectory on $[0, T]$ then there exists $p(\cdot)$ non zero such that the triplet (x, p, u) is solution of the Hamiltonian dynamics:

$$\dot{x} = \frac{\partial H}{\partial p}\,, \qquad \dot{p} = -\frac{\partial H}{\partial x}\,,$$
$$H(x, p, u) = \max_{|v| \leq 1} H(x, p, v) = M(x, p)\,. \tag{11}$$

Moreover, the maximal Hamiltonian M is a nonnegative constant $M = -p_0 \geq 0$ and at the final time T the pair (x, p) satisfies the transversality condition:

$$p(T) \perp T^*_{x(t)}\,\boldsymbol{N}\,. \tag{12}$$

Definition 4. A triplet (x, p, u) solution (11) is called *extremal* and a x-projection of an extremal is called a *geodesic*. Denoting $z = (x, p)$ the symplectic coordinates, an extremal is called *regular* if $u(t) = sign\, H_G(z(t))$ a.e. and *singular* if $H_G(z(t)) = 0$ identically. An extremal is called *exceptional* if the maximized Hamiltonian M is zero. A *BC-extremal* is an extremal satisfying the transversality condition (12). A *switching time* is a time such that the extremal control is discontinuous and a *BC-extremal* is a regular extremal such that the number of switches on $[0, T]$ is finite. We denote respectively by σ_+, σ_-, σ_s, bang arcs associated to $u = +1$, $u = -1$ or $u = u_s$ singular and $\sigma_1\,\sigma_2$ is the *concatenation* of the two arcs σ_1, σ_2.

Definition 5. Taking an open set V of M, the problem (restricted to V) is called *geodesically complete* if, for each pair $x_0,\ x_1 \in V$ there exists a time minimizing geodesics joining x_0 to x_1. Fixing the target to $\boldsymbol{N}$, a *time minimal synthesis* is a (discontinuous) feedback $x \mapsto u^*(x)$ so that the solution of $\dfrac{\mathrm{d}x}{\mathrm{d}t} = X(x) + u^*(x)Y(x)$ is well defined and $u^*(x)$ is the optimal solution to steer x to the target $\boldsymbol{N}$, in minimum time.

Definition 6. Let (z, u_s) be a reference singular extremal of order 2, so that u_s is defined by (9). The associated singular trajectory (x, u_s) is called *strict* if p is unique up to a scalar. In the strict case, singular extremals are said to be *hyperbolic* if $H_F(z)\,\{\{H_G, H_F\}, H_G\}(z) > 0$, *elliptic* if $H_F(z)\,\{\{H_G, H_F\}, H_G\}(z) < 0$. Note that in the *exceptional case*, since $M = 0$, both p and $-p$ can be taken as adjoint vector.

One has the high order Maximum Principle [14].

Proposition 4. Let $(z(\cdot) = (x(\cdot), p(\cdot))$ be a singular extremal on $[0, T]$ and associated to a control which is strictly feasible. Then a necessary time minimizing condition is the *generalized Legendre-Clebsch condition*

$$\frac{\partial}{\partial u}\frac{\mathrm{d}^2}{\mathrm{d}t^2}\frac{\partial H}{\partial u}_{|z(t)} = \left\{\left\{H_G, H_F\right\}, H_G\right\}(z(t)) \geq 0.$$

If the inequality is strict it is called the *strong* generalized Legendre-Clebsch condition.

Remark 2. Reversing the previous inequality leads to a necessary time maximizing condition.

3.3 | Small time classification of regular extremals

One recalls the following result [16].

Definition 7. Recall that σ_+ (respectively σ_-) denotes a bang arc with constant control $u = 1$ (respectively $u = -1$) and σ_s a feasible singular arc. We denote by $\sigma_1\sigma_2$ the arc σ_1 followed by σ_2. The surface $\Sigma : H_G(z) = 0$ is called the *switching surface* and let $\Sigma' \subset \Sigma$ given by $H_G(z) = H_{[G,F]}(z) = 0$. Let $z(\cdot) = (x(\cdot), p(\cdot))$ be a reference curve on $[0, T]$. We note $\Phi(t) = H_G(z(t))$ the switching function, coding the switching times.

Deriving twice Φ with respect to time, one gets:

$$\dot{\Phi}(t) = \{H_G, H_F\}(z(t))$$

and

$$\ddot{\Phi}(t) = \{\{H_G, H_F\}, H_F\}(z(t)) + u(t)\{\{H_G, H_F\}, H_G\}(z(t)) \ . \tag{13}$$

Lemma 1. Assume that t is an *ordinary switching time* that is $\Phi(t) = 0$ and $\dot{\Phi}(t) \neq 0$. Then, near $z(t)$, every extremal projects onto $\sigma_+\sigma_-$ if $\dot{\Phi}(t) < 0$ and $\sigma_-\sigma_+$ if $\dot{\Phi}(t) > 0$.

The situation is more complex for contact of order 2 with Σ.

Definition 8. The case $\Phi(t) = \dot{\Phi}(t) = 0$ and $\ddot{\Phi}(t) \neq 0$ for both $u = \pm 1$ in (13) is called the *fold case* and hence $z(t) \in \Sigma'$. Assume that Σ' is a regular surface of codimension two. We have three cases:

- *parabolic case*: $\ddot{\Phi}_+(t)\,\ddot{\Phi}_-(t) > 0$;
- *hyperbolic case*: $\ddot{\Phi}_+(t) > 0$ and $\ddot{\Phi}_-(t) < 0$;
- *elliptic case*: $\ddot{\Phi}_+(t) < 0$ and $\ddot{\Phi}_-(t) > 0$.

where $\ddot{\Phi}_\varepsilon$, $\varepsilon \in \{-1, 1\}$ is given by (13) with $u = \varepsilon$.

Denote by $u_s(\cdot)$ the singular control of order 2 defined by (9), $z(\cdot) = (\sigma_s, \cdot)$, we assume that the regularity condition $\{\{H_G, H_F\}, H_G\}(z(t)) \neq 0$ holds. The arc σ_s is hyperbolic if $H_F(z(t))\{\{H_G, H_F\}, H_G\}(z(t)) > 0$, elliptic if $H_F(z(t))\{\{H_G, H_F\}, H_G\}(z(t)) < 0$. In the parabolic case, it can be absent or not feasible, that is, $|u_s(t)| > 1$.

We have the following result.

Proposition 5. In the neighborhood of $z(t)$, every extremal projects onto:

- in the parabolic case: $\sigma_+\,\sigma_-\,\sigma_+$ or $\sigma_-\,\sigma_+\,\sigma_-$;
- in the hyperbolic case: $\sigma_\pm\,\sigma_s\,\sigma_\pm$;
- in the elliptic case, every extremal is bang-bang but the number of switches is not uniformly bounded.

3.4 | Classification of the regular syntheses near the terminal manifold using singularity theory

This is the main technical tool of this article, we use the techniques to classify generically the time minimal synthesis[5, 17] near the terminal manifold. Before introducing the results, we present the following properties.

3.4.1 | The role of the transversality condition

Let $x_0 \in \boldsymbol{N}$ and identify locally x_0 to 0 and $\boldsymbol{N}$ to the plane $x_1 = 0$, which divides the space into two neighborhood U_+ and U_- of 0 contained respectively in $x_1 > 0$ and $x_1 < 0$. The cones of admissible directions is given by the convex cone $\boldsymbol{C}$ generated $\{F \pm G\}$, which is strict except in the collinear case. The normal to $\boldsymbol{N}$ can be taken as $n = (1, 0, \dots, 0)^T$. Clearly, in the generic case, the time minimal policy for small time amounts to maximize the $n \cdot \dot{x} = \dot{x}_1$ among the set of all admissible controls, which is precisely the transversality condition. Non generic case occurs when no information is obtained from this condition.

The problem can be classified into the *flat* and *non flat case*. The flat case being when $\boldsymbol{G}$ is everywhere tangent to $\boldsymbol{N}$.

3.4.2 | Concepts of regular synthesis

Take a terminal point x_0 identified to 0 and let U be a small open neighborhood of 0. The terminal manifold $\boldsymbol{N}$ can be locally defined as $\boldsymbol{N} = f^{-1}(0)$, where f is a submersion from U onto a neighborhood of 0 in $\mathbb{R}$. The set of triples (F, G, f) is endowed with the $\mathbb{C}^\infty$–Whitney topology and we denote by $j^n F(x_0)$ (resp. $j^n G(x_0)$, $j^n f(x_0)$) the n-jet of F (resp. G, f) obtained by taking the Taylor expansion at x_0. We say that the triplet (F, G, f) has at x_0 a singularity of codimension i if $\left(j^n F(x_0),\, j^n G(x_0),\, j^n f(x_0)\right) \in \Sigma_i$, a semialgebraic submanifold of codimension i in the jet space.

The references [5, 17] classify up to codimension ≤ 2 the local time minimal syntheses in a neighborhood U of $\boldsymbol{N}$ by estimating up to any order the switching and cut loci.

Actually, the optimal control u^* not always define on the whole set U since, for some $x \in U$ the target $\boldsymbol{N}$ is not accessible. This can be shown to be related to the exceptional case. It can also happen that u^* is not uniquely defined. The set of such points is called the *splitting locus* and is denoted by L.

If $u^*(x)$ exists and is unique, in the *regular case* $|u^*(x)| = 1$ and U can be partitioned into U^+ where $u^*(x) = 1$ and U^- where $u^*(x) = -1$. In our work, we can compute the subanalytic surface S separating U^+ from U^- and its structure of three kinds.

- *Switching surface:* closure of the set points where u^* is regular but not continuous, denoted by $W_\#$ ($\# \in \{+, -, s\}$) where at a switching point the control is taken right-continuous by convention.
- *Cut locus:* if σ is a minimizing curve, it will be defined on an interval $[T, 0]$, with $T < 0$, integrating backwards from the final point on $\boldsymbol{N}$ and the cut-locus is the closure of the set of cut points where the trajectory loses its optimality status. It is denoted by C and contains the splitting locus.
- *Singular locus:* it is foliated by optimal singular arcs and denoted by Γ_s. Recall that if $u_s \in]-1, +1[$ the singular trajectory σ_s is strictly feasible, if $u_s \in \{-1, +1\}$ it is saturated.

To simplify the estimates of the previous strata, one use semi-normal forms for the restricted actions of the feedback group related to local diffeomorphisms φ preserving 0 and exchange of u into $-u$, so that one can identified σ_+ to σ_- in the classification.

3.4.3 | Description of the local syntheses

Next we present a dictionary of syntheses describing the classification of syntheses up to the codimension one. They are represented as $2d$–pictures, thanks to the existence in those small codimension case to the C^0*-foliations of the syntheses in invariant planes*. One distinguishes between the flat case (see Figures 9–11) and non flat case (see Figures 4–8).

A much more complete dictionary can be found in [5, 17], in particular to deal with generic $3d$-systems, where more complicated phenomenon can occur due to *non-existence of foliations by* $2d$*–planes*. Estimates of the strata are given related to the jet spaces of the triples (X, Y, f) at $x_0 = 0$. The semi-algebraic sets Σ_i are described and the syntheses can be described using Lie algebraic computations only. Applications to our specific problem can be given by gluing such syntheses, see [6].

3.5 | The digital case *versus* the permanent case

In the digital case, we divide $[0, T]$ into $0 = t_0 < t_1 < \dots < t_n < T$ and on each subinterval $[t_i, t_{i+1}]$ the control is a constant u_i, $|u_i| \leq 1$. The digital aspect is the interpulse constraint $t_{i+1} - t_i \geq I_m$ with fixed $I_m \geq 0$. Hence, such control is represented by a sequence $\delta = \left(u_0, \dots, u_n, t_1, \dots, t_n\right)$. Assume that δ is optimal. The set of admissible perturbations $\bar{\delta} = \left(\bar{u}_0, \dots, \bar{u}_n, \bar{t}_1, \dots, \bar{t}_n\right)$ decomposes into:

- L^∞-admissible perturbations if there exists, for each $i = 0, \dots, n$, $\bar{\varepsilon} > 0$ such that $u_i + \varepsilon \bar{u}_i \in [-1, +1]$ for all $0 \leq \varepsilon \leq \bar{\varepsilon}$.

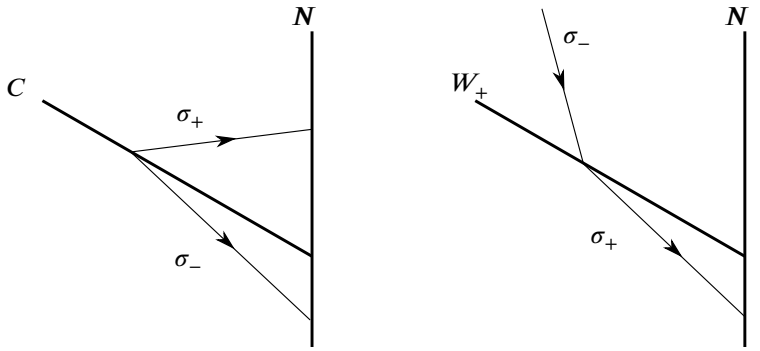

FIGURE 4 Non flat case. Generic ordinary switching point.

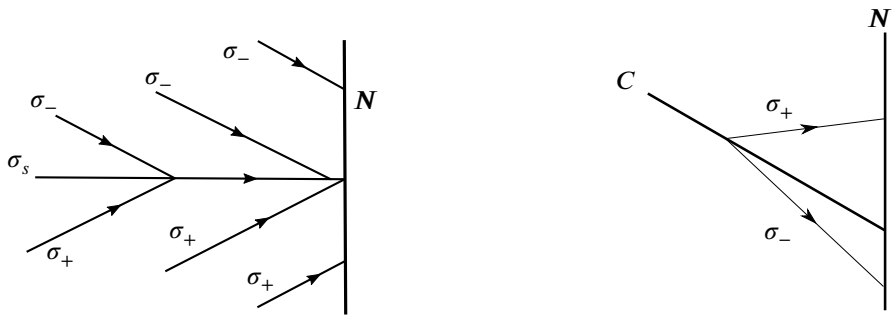

FIGURE 5 Non flat case. Generic hyperbolic case.

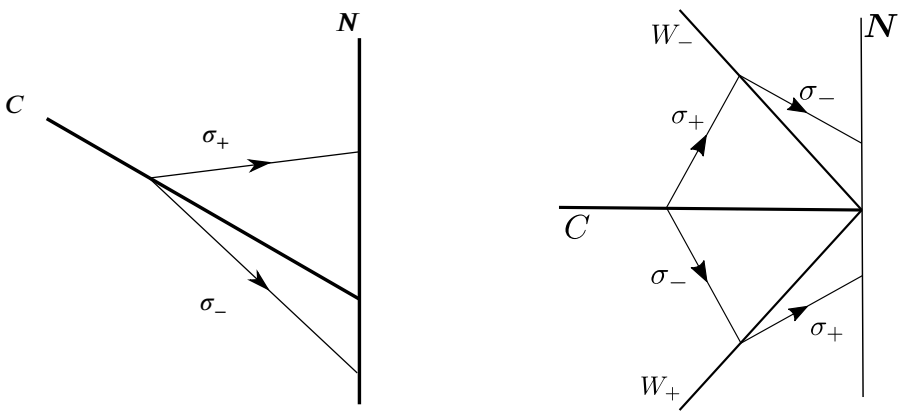

FIGURE 6 Non flat case. Generic elliptic case.

- L^1-admissible perturbations $\bar{t}_i \in \mathbb{R}$ of t_i if there exists $\bar{\varepsilon} > 0$ such that $\left(t_i + \varepsilon \bar{t}_i\right) - t_{i-1} \geq I_m$ and $t_{i+1} - \left(t_i + \varepsilon \bar{t}_i\right) \geq I_m$ for all $0 \leq \varepsilon \leq \bar{\varepsilon}$, for $i = 1, \ldots, n-1$ while for $i = n$ only $\left(t_n + \varepsilon \bar{t}_n\right) - t_{n-1} \geq I_m$ holds.

Each admissible perturbation provides a tangent solution of the linear differential equation:

$$\dot{w}(t) = \left(\frac{\partial F}{\partial x} + u_\delta \frac{\partial G}{\partial x}\right)\left(x_\delta(t)\right) \cdot w(t), \tag{14}$$

where (x_δ, u_δ) denotes the control trajectory pair on $[0, T]$ given by δ.

If φ denotes the Mayer cost to be maximized, from optimality one gets

$$\varphi\left(x_\delta(t)\right) - \varphi\left(x_{\bar{\delta}}(t)\right) \geq 0\,,$$

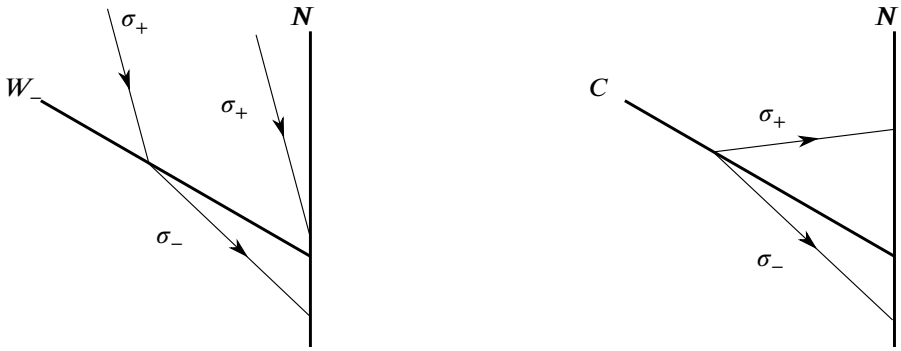

FIGURE 7 Non flat case. Generic parabolic case.

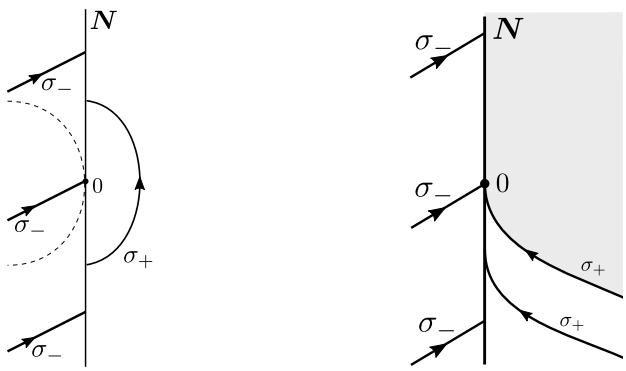

FIGURE 8 Non flat case. Generic exceptional case.

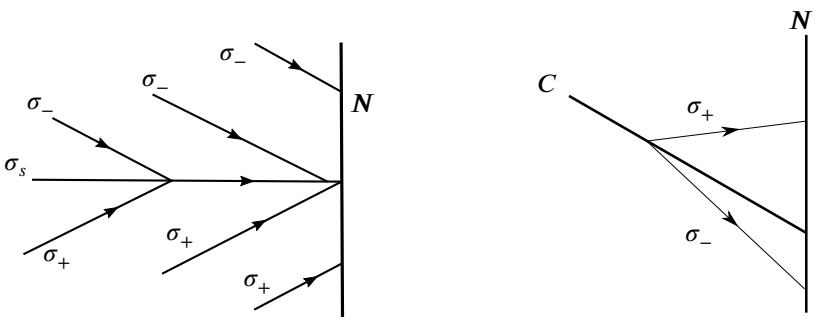

FIGURE 9 Flat case. Hyperbolic case *(left)* and elliptic case *(right)*.

for every admissible perturbation. Taking the limit as $\varepsilon \to 0^+$, one obtains the condition

$$\frac{\partial \varphi}{\partial x}\left(x_\delta(T)\right) \cdot w(T) \geq 0.$$

We introduce the adjoint equation

$$\dot{p}(t) = -p(t)\left(\frac{\partial F}{\partial x} + u_\delta \frac{\partial G}{\partial x}\right)\left(x_\delta(t)\right),$$

where $p(\cdot)$ is written as a row-vector with terminal condition

$$p(T) = -\frac{\partial \varphi}{\partial x}\left(x_\delta(T)\right).$$

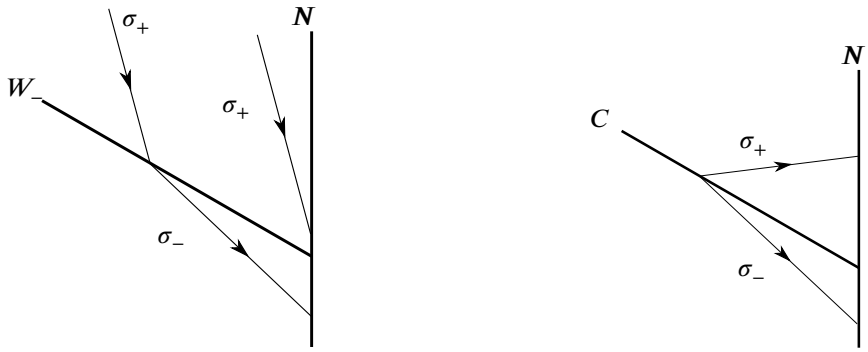

FIGURE 10 Flat case. Generic parabolic case

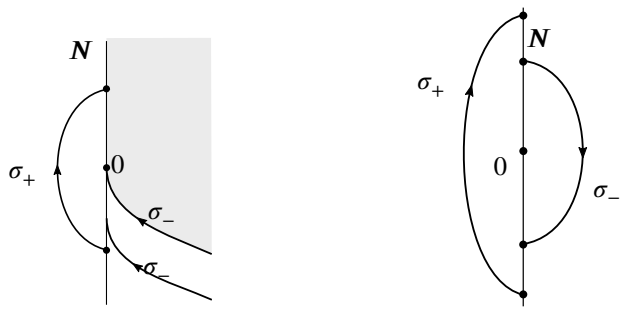

FIGURE 11 Flat case. Generic exceptional case.

Observe that for each solution $w(t)$ of the variational equation one has $p(t) \cdot w(t) = 0$. Moreover, denoting by $\Phi(\cdot, \cdot)$ the state transition matrix associated to the linear system (14), one has

$$w(T) = \Phi(T, s)\, w(s),$$
$$p(s) = p(T)\, \Phi(T, s)^T .$$

In particular, for L^∞-perturbations one gets.

Proposition 6. In the sampled-data case, with fixed interpulses, one gets the necessary optimality condition

$$\int_{t_i}^{t_{i+1}} \big(p(s)G(x_\delta(t))\big)\, \delta u_i \leq 0\,,$$

for each admissible variation δu_i.

Similarly, one can derive the necessary conditions with free sampling times.

This leads to the so-called (indirect) Pontryagin type necessary optimality conditions for the sampled-data case. The numerical implementation of such condition is difficult and this requires to a more direct treatment.

3.6 | Optimal sampled-data control and model predictive control (MPC) algorithm

In the optimal sampled-data control frame, the problem leads to consider a finite dimensional problem of the form:

$$\min_{\delta}\ J(x_0, \delta)\,,$$

where x_0 is the initial condition and $\delta = \big(t_1, \dots, t_n, u_0, \dots, u_{n-1}\big)$ represents the finite dimensional set of controls associated to the choice of time sampling and control amplitudes of each sampling and constraints are given by the interpulses constraints $t_i - t_{i-1} \geq I_m$ and each $u_i \in [0, 1]$.

The direct approach amounts to apply an optimization algorithm to search for the optimum. In our study, it will be coupled with the following MPC approach.

MPC algorithm.

One starts with the initial state x_0 at time t_0 which practically can be estimated by $\hat{x}_0$. We fix an horizon of length k and we apply the optimization algorithm over the subset of admissible controls $\mathcal{C}$ of $\mathbb{R}^{2k}$. This routine leads to compute the optimization sequences

$$\delta_k^* = \left(t_1^*, \dots, t_k^*, u_0^*, \dots, u_{k-1}^*\right), \quad t_i^* - t_{i-1}^* \geq I_m$$

and we apply to the dynamics (t_1^*, u_1^*) to get at time t_1^* the response $x^*(t_1^*)$. We iterate the construction replacing t_0 by t_1^* and x_0 by $x^*(t_1^*)$ (see Fig. 12).

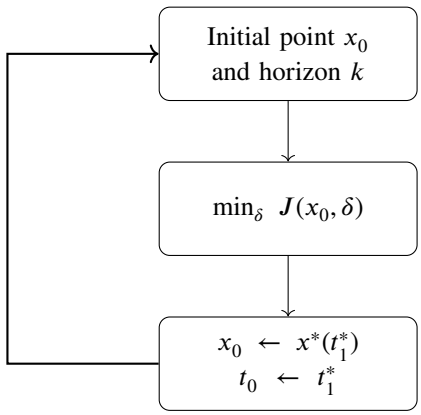

FIGURE 12 MPC algorithm with horizon of length k.

4 | COMPUTATIONS AND PRELIMINARY RESULTS ON THE GENERALIZED LOTKA–VOLTERRA MODEL

We start with the control system (4) with either an antibiotic or a probiotic agent. Using dimensionless coordinates, $x_i \leftarrow x_i/x_i^*$, $i = 1, 2$ where x_i^* are the coordinates of the persistent equilibrium, the persistent equilibrium is normalized to $(1, 1)$ and substituting $\boldsymbol{\epsilon}$ to $\rho = (\rho_1, \rho_2)^\intercal$ according to $\rho = -A^{-1}\boldsymbol{\epsilon}$ leads to the system:

$$\dot{x} = \operatorname{diag} x \, A \, (x - \mathbf{1} - u\rho)$$

with $\mathbf{1} = (1, 1)^\intercal$. Therefore the vector fields used in this section resulting from this normalization are :

$$X = \operatorname{diag} x \, A \, (x - \mathbf{1}), \quad Y = -\operatorname{diag} x \, A \, \rho.$$

4.1 | Geometric analysis in the $2d$–case

4.1.1 | Equilibria and the collinear set

The collinear set $\mathcal{C}$ is one of the main feedback invariant related to the computations of free equilibria with no treatment $u = 0$ and forced equilibria with maximal dosing $u = 1$. This set is the one dimensional algebraic variety projection on the state-space of the set

$$\mathcal{C} = \{(x, u) \in \mathbb{R}^2 \times \mathbb{R}, \; \exists u \text{ such that } X(x) + u\,Y(x) = 0\}. \tag{15}$$

Moreover the control u has to be feasible : $u \in [0, 1]$. This projection is also given by the determinantal variety: $\det(X(x), Y(x)) = 0$:

$$x_1 x_2 \det A \left(\rho_1(x_2 - 1) - \rho_2(x_1 - 1)\right) = 0,$$

and it consists of the half-line $\mathcal{C} \; : \; x_2 = 1 + \rho_2/\rho_1(x_1 - 1)$ in the positive orthant $x_1, x_2 \geq 0$. The control along $\mathcal{C}$ such that $X(x) + u_e(x)\,Y(x) = 0$ is given by $u_e(x) = (x_1 - 1)/\rho_1 \in [0, 1]$.

At a point $x_e = (x_{1e}, x_{2e}) \in C$ associated to the control u_e, the Jacobian matrix

$$J = \frac{\partial}{\partial x}\left(X(x) + u\,Y(x)\right)_{|x=x_e(x),u=u_e(x)} \tag{16}$$

has the two eigenvalues

$$\left(\lambda \pm \sqrt{\lambda^2 + 4\det A\rho_1 x_{1e}(\rho_2(1-x_{1e}) - \rho_1)}\right)/2\rho_1,$$

where $\lambda = a_{22}(\rho_1 - \rho_2) + x_{1e}(\rho_1 a_{11} + \rho_2 a_{22})$.

The persistent equilibrium point $x_e^0 = (1,1)$ has eigenvalues

$$(a_{11} + a_{22})/2 \pm \sqrt{(a_{11} + a_{22})^2 - 4\det A}\,/2$$

and the forced equilibrium point $x_e^1 = (1+\rho_1, 1+\rho_2)$ associated to $u_e = 1$ has eigenvalues

$$((1+\rho_1)a_{11} + (1+\rho_2)a_{22})/2 \pm \sqrt{((1+\rho_1)a_{11} + (1+\rho_2)a_{22})^2 - 4(1+\rho_1)(1+\rho_2)\det A}\,/2.$$

We obtain the following Proposition:

Proposition 7. Assume $\rho_1, \rho_2 > -1$ and introduce $\alpha = 1+\rho_1, \beta = 1+\rho_2$. The forced equilibrium x_e^1 is in the positive orthant and

- if $\det A < 0$ and $a_{11} \neq -a_{22}$, $\alpha a_{11} \neq -\beta a_{22}$ then x_e^0 and x_e^1 are saddle points.
- if $\det A > 0$, then x_e^0 and x_e^1 are either nodes or spiral points. More precisely, if moreover
  - $a_{11}a_{22} \geq 2\det A$, then x_e^0 and x_e^1 are both nodes.
  - $a_{11} = -a_{22}$, then x_e^0 is a center. If moreover $\rho_1 = \rho_2$, then x_e^1 is a center.
  - $a_{11}a_{22} \leq 2\det A$, $(\alpha^2+\beta^2)(1 - a_{11}a_{22}/\det A) - 2\alpha\beta < 0$, then if x_e^0 is a focus, then x_e^1 is a focus.

Proof. The forced equilibrium $x_e^1 = (\alpha, \beta)$ is in the positive orthant. If $\det A < 0$, the statement is clear. If $\det A > 0$ and $a_{11}a_{22} \geq 2\det A$ then $(a_{11}+a_{22})^2 - 4\det A \geq 0$ and denoting $m = \min(\alpha,\beta)$, we have:

$$(\alpha a_{11} + \beta a_{22})^2 - 4\det A\alpha\beta \geq m^2(a_{11}^2 + a_{22}^2 + 2a_{11}a_{22}\beta\alpha/m^2 - 4\det A\beta\alpha m^2 \geq 2m^2(1-\beta\alpha/m^2)(2\det A - a_{11}a_{22}) \geq 0,$$

and x_e^1 is a node. The last item follows from

$$(\alpha a_{11} + \beta a_{22})^2 - 4\det A\alpha\beta \leq (\alpha^2+\beta^2)(x^2+y^2) - 4\det A\alpha\beta \leq 2\det A((\alpha^2+\beta^2)(1 - a_{11}a_{22}/\det A) - 2\alpha\beta) \leq 0.$$

□

4.1.2 | Singular locus in the $2d$–case

Singular trajectories are located on the set

$$\mathcal{S} : \det([Y,X](x), Y(x)) = 0,$$

which is given by:

$$\mathcal{S} : x_1 x_2 \det A\left(\rho_1 x_2\left(\rho_1 a_{21} + \rho_2 a_{22}\right) - \rho_2 x_1\left(\rho_1 a_{11} + \rho_2 a_{12}\right)\right),$$

and corresponds to the half-line $x_2 = x_1\,\rho_2\left(\rho_1 a_{11} + \rho_2 a_{12}\right)/\left(\rho_1\left(\rho_1 a_{21} + \rho_2 a_{22}\right)\right)$ in the positive orthant.

The intersection of $\mathcal{S}$ and C is therefore:

$$x_{se} = \left(\frac{(\rho_1-\rho_2)\left(\rho_1 a_{21} + \rho_2 a_{22}\right)}{\rho_2\left(\rho_1 a_{11} - \rho_1 a_{21} + \rho_2 a_{12} - \rho_2 a_{22}\right)}, \frac{(\rho_1-\rho_2)\left(\rho_1 a_{11} + \rho_2 a_{12}\right)}{\rho_1\left(\rho_1 a_{11} - \rho_1 a_{21} + \rho_2 a_{12} - \rho_2 a_{22}\right)}\right). \tag{17}$$

Now we investigate the existence of a singular control in the optimal policy near the point x_{se}. Outside the set C, (X,Y) is a frame and we write

$$[Y,X](x) = \alpha(x)X(x) + \beta(x)Y(x),$$

where

$$\alpha(x) = \frac{\det([Y,X],Y)(x)}{\det(X,Y)(x)} = \frac{\rho_1 x_2\left(\rho_1 a_{21} + \rho_2 a_{22}\right) - \rho_2 x_1\left(\rho_1 a_{11} + \rho_2 a_{12}\right)}{\rho_1(x_2-1) - \rho_2(x_1-1)}, \quad \beta(x) = \frac{\det(X,[Y,X])(x)}{\det(X,Y)(x)}.$$

Using this decomposition to compute Lie brackets of length 3 we obtain

$$[[Y,X],Y] = [\alpha X, Y] + [\beta Y, Y] = X\nabla\alpha^{\intercal}Y + \alpha[X,Y] + Y\nabla\beta^{\intercal}Y = (-\alpha^2 + Y\cdot\nabla\alpha)X + (-\alpha\beta + Y\cdot\nabla\beta)Y \tag{18}$$

and

$$[[Y,X],X] = [\alpha X, X] + [\beta Y, X] = (X\cdot\nabla\alpha + \alpha\beta)X + (X\cdot\nabla\beta + \beta^2)Y.$$

Two necessary conditions are (i) the singular control is admissible i.e. $u_s \in [0,1]$ and (ii) the strong generalized Legendre-Clebsch condition is satisfied.

The singular control denoted u_s is computed using

$$p\cdot\left([[Y,X],X](x) + u_s\,[[Y,X],Y](x)\right) = 0$$

and since p is also orthogonal to $Y(x)$ on $\mathcal{S}$, we obtain for $x \in \mathcal{S}\setminus\{x_{se}\}$

$$u_s = -\frac{\det(Y,[[Y,X],X])}{\det(Y,[[Y,X],Y]])} = -\frac{X\cdot\nabla\alpha}{Y\cdot\nabla\alpha} = \frac{x_1\left(\rho_1 a_{21} + \rho_2 a_{12}\right)}{\rho_1\left(\rho_1 a_{21} + \rho_2 a_{22}\right)} + \frac{-a_{11} - a_{12} + a_{21} + a_{22}}{\rho_1 a_{11} - \rho_1 a_{21} + \rho_2 a_{12} - \rho_2 a_{22}}$$

and the value of u_s at x_{se} is

$$u_s(x_{se}) = \frac{-\rho_1\rho_2 a_{11} + \rho_1\left(\rho_1 a_{21} + \rho_2 a_{22}\right) - a_{12}\rho_2^2}{\rho_1\rho_2\left(\rho_1 a_{11} - \rho_1 a_{21} + \rho_2 a_{12} - \rho_2 a_{22}\right)}.$$

On $\mathcal{S}$, we have $\alpha = 0$, $p\cdot Y = 0$ and from (18) the strong generalized Legendre-Clebsch condition yields

$$0 < p\cdot[[Y,X],Y] = p\cdot(Y\cdot\nabla\alpha)X,$$

which is equivalent to $Y\cdot\nabla\alpha > 0$ (we oriented p such that $p\cdot X \geq 0$). Geometrically this means that Y has to point in the region where $\alpha > 0$.

4.2 | Computation in the higher dimensional cases

4.2.1 | Classification of singular trajectories

In the $N \geq 3$ dimensional case the classification of singular trajectories is a very rich problem as illustrated by the 3d-case that we present next.

Let (X,Y) be a pair of vector fields and we introduce the following determinants :

- $D^{X,Y} = \det(Y,[Y,X],[[Y,X],Y])$,
- $D'^{X,Y} = \det(Y,[Y,X],[[Y,X],X])$,
- $D''^{X,Y} = \det(Y,[Y,X],X)$.

Proposition 8. The singular trajectories of order 2 are defined by the dynamics:

$$\dot{x} = X_s(x) = X(x) - \frac{D'(x)}{D(x)}Y(x)$$

on $\mathbb{R}^3$.

Proof. In the 3d-case, the adjoint vector p can be eliminated using the relations:

$$p\cdot Y(x) = p\cdot[Y,X](x) = p\cdot\left([[Y,X],X](x) + u_s\,[[Y,X],Y](x)\right),$$

where u_s is the singular control. Hence it is given by the feedback: $u_s = -\frac{D'(x)}{D(x)}$. □

Proposition 9. In dimension 3, the feedback group acts as change of coordinates only and $\lambda_1 : (X,Y) \mapsto X_s(x) = X(x) - \frac{D'(x)}{D(x)}Y(x)$ is a covariant i.e. the following diagram is commutative:

$$\begin{array}{ccc} (X,Y) & \xrightarrow{\lambda_1} & X_s \\ {\scriptstyle G_f}\downarrow & \circlearrowleft & \downarrow{\scriptstyle G_f} \\ (X',Y') & \longrightarrow & X'_s \end{array}.$$

Proof. Direct computations give us:

$$D^{\phi*X,\phi*Y}(x) = \det\left(\frac{\partial\phi}{\partial x}\right) D^{X,Y}(\phi^{-1}(x)), \qquad D'^{\phi*X,\phi*Y}(x) = \det\left(\frac{\partial\phi}{\partial x}\right) D'^{X,Y}(\phi^{-1}(x)),$$
$$D''^{\phi*X,\phi*Y}(x) = \det\left(\frac{\partial\phi}{\partial x}\right) D''^{X,Y}(\phi^{-1}(x)), \qquad D^{X+\alpha Y,\beta Y}(x) = \beta^4 D^{X,Y}(x),$$
$$D'^{X+\alpha Y,\beta Y}(x) = \beta^3 D'^{X,Y}(x), \qquad D''^{X+\alpha Y,\beta Y}(x) = \beta^2 D''^{X,Y}(x).$$

Hence λ_1 is a covariant. □

Moreover we have:

Corollary 1. The sets $D'' = 0$, $DD'' > 0$ and $DD'' < 0$, foliated respectively by exceptional, hyperbolic and elliptic singular arcs, are invariant for the solutions of $\dot{x} = X_s(x)$.

Proof. We use the relation

$$(u \wedge v) \cdot w = \det(u, v, w)$$

to deduce

$$(Y \wedge [Y, X]) \cdot X = \det(Y, [Y, X], X)$$
$$(Y \wedge [Y, X]) \cdot Y = \det(Y, [Y, X], Y)$$

to classify singular trajectories with the strong generalized Clebsch condition

$$(p \cdot X(x))(p \cdot [[Y, X], X](x)) > 0$$

with $p \cdot Y(x) = p \cdot [Y, X](x) = 0$. This gives the determinantal conditions. □

4.2.2 | Computations for the GLV–model.

In the 3–dimensional GLV–model, the expressions of D, D', D'' in the original coordinates are:

$$\begin{aligned}
D(x)/x_1x_2x_3 = {} & \left(\varepsilon_1^2 x_1 a_{21} + \varepsilon_1\left(\varepsilon_2\left(x_2a_{22} - x_1a_{11}\right) + \varepsilon_3x_3a_{23}\right) - \varepsilon_2\left(\varepsilon_2x_2a_{12} + \varepsilon_3x_3a_{13}\right)\right) \\
& \left(\varepsilon_1^2x_1a_{31} + \varepsilon_2^2x_2a_{32} + \varepsilon_3^2x_3a_{33}\right) + \left(\varepsilon_1^2x_1a_{11} + \varepsilon_2^2x_2a_{12} + \varepsilon_3^2x_3a_{13}\right)\left(\varepsilon_2^2x_2a_{32} + \varepsilon_3\varepsilon_2\left(x_3a_{33} - x_2a_{22}\right)\right. \\
& \left. - \varepsilon_3^2x_3a_{23} + \varepsilon_1x_1\left(\varepsilon_2a_{31} - \varepsilon_3a_{21}\right)\right) - \left(\varepsilon_1^2x_1a_{21} + \varepsilon_2^2x_2a_{22} + \varepsilon_3^2x_3a_{23}\right) \\
& \left(\varepsilon_1^2x_1a_{31} + \varepsilon_1\left(\varepsilon_2x_2a_{32} + \varepsilon_3\left(x_3a_{33} - x_1a_{11}\right)\right) - \varepsilon_3\left(\varepsilon_2x_2a_{12} + \varepsilon_3x_3a_{13}\right)\right),
\end{aligned}$$

$$\begin{aligned}
D'(x)/x_1x_2x_3 = {} & \left(-\varepsilon_1^2x_1\, a_{21} + \varepsilon_1\left(\varepsilon_2\left(x_1a_{11} - x_2a_{22}\right) - \varepsilon_3x_3a_{23}\right) + \varepsilon_2\left(\varepsilon_2x_2a_{12} + \varepsilon_3x_3a_{13}\right)\right) \\
& \left(\varepsilon_2x_2\big(x_1a_{12}a_{31} - a_{32}\big(x_1a_{21} + x_3\big(a_{23} - a_{33}\big) + r_2\big)\big) - \varepsilon_1x_1\big(r_1a_{31} + x_3\left(a_{13} - a_{33}\right)a_{31}\right. \\
& \left. + x_2\big(a_{12}a_{31} - a_{21}a_{32}\big)\big) + \varepsilon_3x_3\left(-r_3a_{33} + x_1a_{31}\left(a_{13} - a_{33}\right) + x_2a_{32}\left(a_{23} - a_{33}\right)\right)\right) \\
& + \left(\varepsilon_2^2\left(-x_2\right)a_{32} + \varepsilon_3\varepsilon_2\left(x_2a_{22} - x_3a_{33}\right) + \varepsilon_3^2x_3a_{23} + \varepsilon_1x_1\left(\varepsilon_3a_{21} - \varepsilon_2a_{31}\right)\right) \\
& \Big(-\varepsilon_1x_1\left(r_1a_{11} + x_2a_{12}\left(a_{11} - a_{21}\right) + x_3a_{13}\left(a_{11} - a_{31}\right)\right) + \varepsilon_2x_2\big(x_3a_{13}a_{32} - a_{12}\big(x_1\left(a_{21} - a_{11}\right) \\
& + x_3a_{23} + r_2\big)\big) - \varepsilon_3x_3\left(a_{13}\left(x_1\left(a_{31} - a_{11}\right) + x_2a_{32} + r_3\right) - x_2a_{12}a_{23}\right)\Big) \\
& - \left(\varepsilon_1^2\left(-x_1\right)a_{31} + \varepsilon_1\left(\varepsilon_3\left(x_1a_{11} - x_3a_{33}\right) - \varepsilon_2x_2a_{32}\right) + \varepsilon_3\left(\varepsilon_2x_2a_{12} + \varepsilon_3x_3a_{13}\right)\right) \\
& \Big(\varepsilon_1x_1\left(x_3a_{23}a_{31} - a_{21}\left(x_3a_{13} + x_2\left(a_{12} - a_{22}\right) + r_1\right)\right) + \varepsilon_2x_2\big(-r_2a_{22} + x_1a_{21}\left(a_{12} - a_{22}\right) \\
& + x_3a_{23}\left(a_{32} - a_{22}\right)\big) + \varepsilon_3x_3\left(x_1a_{13}a_{21} - a_{23}\left(x_1a_{31} + x_2\left(a_{32} - a_{22}\right) + r_3\right)\right)\Big),
\end{aligned}$$

$$\begin{aligned}
D''(x)/x_1x_2x_3 = {} & \left(-\varepsilon_1^2x_1a_{21} + \varepsilon_1\left(\varepsilon_2\left(x_1a_{11} - x_2a_{22}\right) - \varepsilon_3x_3a_{23}\right) + \varepsilon_2\left(\varepsilon_2x_2a_{12} + \varepsilon_3x_3a_{13}\right)\right) \\
& \left(x_1a_{31} + x_2a_{32} + x_3a_{33} + r_3\right) + \big(-\varepsilon_2^2x_2a_{32} + \varepsilon_3\varepsilon_2\left(x_2a_{22} - x_3a_{33}\right) + \varepsilon_3^2x_3a_{23} + \varepsilon_1x_1\big(\varepsilon_3a_{21} \\
& - \varepsilon_2a_{31}\big)\big)\left(x_1a_{11} + x_2a_{12} + x_3a_{13} + r_1\right) + \left(\varepsilon_1^2x_1a_{31} + \varepsilon_1\left(\varepsilon_2x_2a_{32} + \varepsilon_3\left(x_3a_{33} - x_1a_{11}\right)\right)\right. \\
& \left. - \varepsilon_3\left(\varepsilon_2x_2a_{12} + \varepsilon_3x_3a_{13}\right)\right)\left(x_1a_{21} + x_2a_{22} + x_3a_{23} + r_2\right).
\end{aligned}$$

4.3 | Numerical methods

We consider the controlled system $\dot{x} = X + u\,Y$, $X = \mathrm{diag}\, x\, A\ (x - \mathbf{1})$, $Y = -\mathrm{diag}\, x\, A\, \rho$. The aim is to reach in minimum time an healthy region defined by $\boldsymbol{N}(x) \leq 0$ and the formulation of this class of problems is

$$(P) \qquad \begin{array}{l} \min_{u(\cdot)}\ \boldsymbol{N}(x(T)) \\ \dot{x}(t) = X(x(t)) + u(t)\,Y(x(t)),\ u(t) \in [0,1],\ a.e.\ t \in [0,T] \\ x(0) = x_0 \text{ (given)}. \end{array}$$

We provide numerical results from a standard direct approach via the Bocop software (see https://www.bocop.org/) and an intuitive model predictive control method described hereafter.

Direct method

It is usually a quite robust method with respect to the initialization, easy to implement but the method does not exploit the geometric properties of the problem, which give the structure of the optimal control. The method goes as follows. Discretizing the state and the control spaces for (P), we obtain a nonlinear finite optimization problems where the derivatives are computed using automatic differentiation and the optimization variables are the values of the control at each time step. Then a primal dual interior point algorithm is used to solve this optimization problem.

Model predictive control method

While the direct method discretizes the problem on the whole interval of time, which may be inefficient, a model predictive control (MPC) method solves iteratively finite dimensional optimization problems of smaller sizes i.e. on a reduced time interval. In terms of the problem (P), we consider an iterative variable x_c, standing for the current state of the system and initialized to x_0. We solve iteratively optimal control problems of the form

$$(P') \qquad \begin{array}{l} \min_{u_1,\dots,u_h \in [0,1]}\ \boldsymbol{N}(x(t_h)) \\ \dot{x}(t) = X(x(t)) + u_i\,Y(x(t)),\ \ t \in [t_i, t_{i+1}],\ i = 0,\dots,h-1 \\ x(0) = x_c \end{array}$$

where h is the horizon and $0 = t_0 < t_1 < \cdots < t_h$ are given fixed times.

Therefore the main steps of our MPC algorithm are:

1. *Initialization :*
   - horizon : t_h,
   - Number of controls on $[0, t_h]$: h,
   - outer time step : $\delta \ll t_h$,
   - current state state $x_c = x_0$,
   - h optimization variable : $u = (u_1, \dots, u_h)$,
   - threshold $\eta > 0$.
2. *Iterations :* While $\boldsymbol{N}(x_c) > \eta$
   $u \leftarrow \min(P')$
   $x_c \leftarrow x(\delta; x_c, u_1)$: solution of $\dot{x}(t) = X(x(t)) + u_1\,Y(x(t))$ at time $t = \delta$ starting at x_c at time 0.

This algorithm is implemented in the WOLFRAM LANGUAGE : inside the conditional loop, solutions of (P') are computed with the routine FINDMINIMUM based on an interior point method and the point $x(\delta; x_c, u_1)$ is computed with the routine NDSOLVEVALUE based on an explicit Runge–Kutta scheme.

4.3.1 | Two dimensional case

In this case, the geometric computations were presented in Section 4.1. We make further normalization to obtain the following geometric picture:

- the persistent equilibrium located at $(1,1)$ is a node,
- the collinearity locus $\mathcal{C}$ intersects the singular locus $\mathcal{S}$ at x_{es} (given by (17)),
- the singular control is admissible at x_{es} and the strong generalized Legendre-Clebsch condition is satisfied in a half–neighborhood of x_{es},

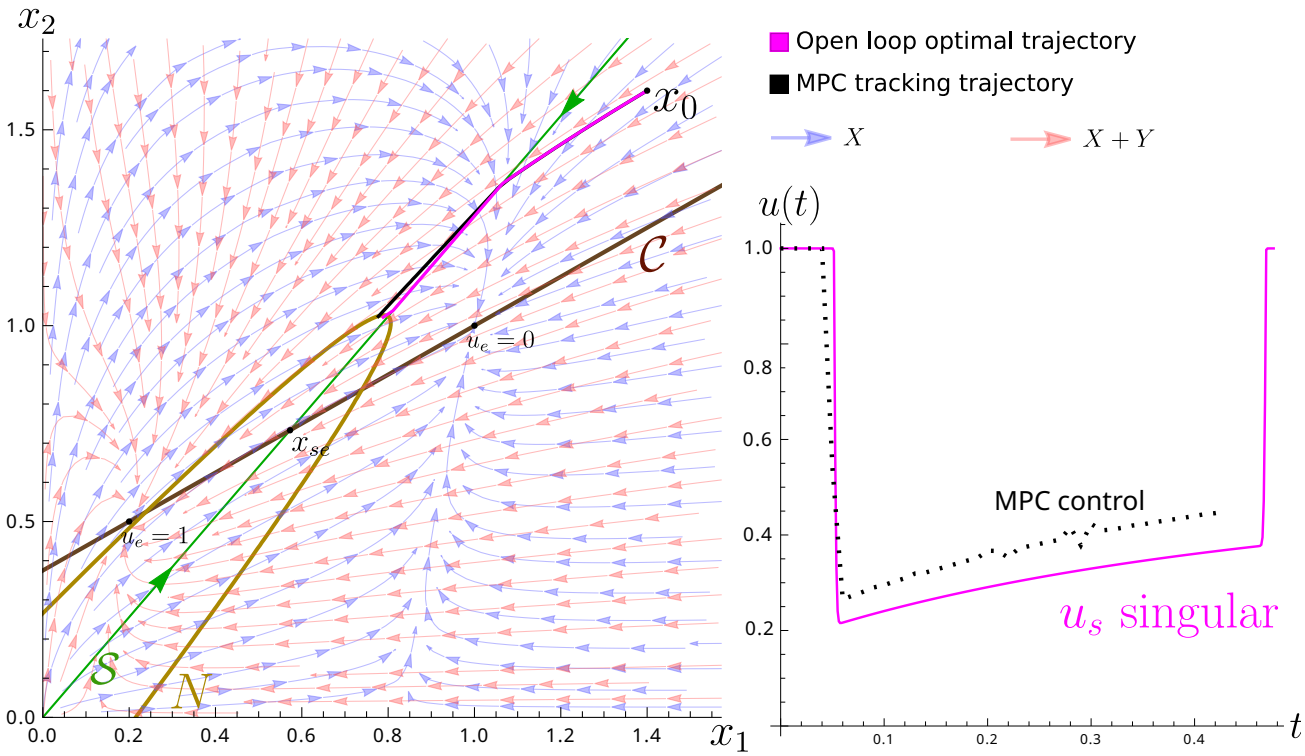

FIGURE 13 Geometric picture corresponding to Example 1. *(left)* The trajectory $x_0 = (7/5, 8/5)$ obtained with a direct method is bang–singular–bang (continuous line) and the MPC trajectory (dashed line) seems to reproduce the singular behavior. *(right)* Time evolution of the control for the direct and MPC methods.

- singular trajectories go toward x_{es} for positive times,
- the boundary of the healthy region $\boldsymbol{N}(x) \leq 0$ is the parabola of equation

$$h\left(P.(x - x_S)\right) = 0, \tag{19}$$

where $h(x_1, x_2) = x_2 - x_1^2$, $P = \begin{pmatrix} \mu & \nu \\ -1 & \nu\mu \end{pmatrix}$ with $\mu = \frac{\rho_2(\rho_1 a_{11} + \rho_2 a_{12})}{\rho_1(\rho_1 a_{21} + \rho_2 a_{22})}$ and $\nu \in \mathbb{R}$, $x_S \in \mathbb{R}^2$ are parameters precised below.

We examine two instances of the problem $(\boldsymbol{P})$ by choosing the values of the parameters thanks to Proposition 7.

Example 1. In this example, $A = \begin{pmatrix} -6 & 1 \\ -2 & -1 \end{pmatrix}$, $\rho_1 = -4/5$, $\rho_2 = -1/2$ and the persistent equilibrium is an attracting focus. The parabola $\boldsymbol{N}$ is defined by (19) with $\nu = -1/20$ and x_S is the point $\mathcal{S} \cap \{x_1 = 0.8\}$ and x_0 is chosen so that $\boldsymbol{N}$ can be reached with bang and singular arcs, see Fig.13. Note that we do not expect the optimal trajectory to cross the collinearity set $\mathcal{C}$.

The direct method gives a bang–singular–bang solution depicted in Fig.13. In the same figure, the model predictive control trajectory with an horizon $t_h = 1$, $h = 4$ seems to faced with a "singular behavior" as in the permanent case.

Example 2. We take $A = \begin{pmatrix} -13 & 18 \\ 12 & -20 \end{pmatrix}$, $\rho_1 = -11/20$, $\rho_2 = 7/10$ and the persistent equilibrium is an attracting node.

(a) in this example, we take $x_0 = (3/2, 1/5)$ and $\boldsymbol{N}$ is the parabola (19) defined by $\nu = 1/6$, x_S is the point $\mathcal{C} \cap \{x_1 = 0.5\}$ translated by $(0.1, 0)$. $\boldsymbol{N}$ is accessible from x_0 with bang and singular arcs and we do not expect the collinearity set to play any role, see Fig.14 (left). The trajectories for both methods differ significantly from each other: the direct method gives a bang–bang–singular–bang solution while the MPC trajectory with $h = 4$ reaches $\boldsymbol{N}$ with a bang arc followed by an arc with intermediate control values.

(b) Here we choose $x_0 = (3/2, 1/5)$ and $\boldsymbol{N}$ is the parabola (19) defined by $\nu = 1/6$, x_S is the point $\mathcal{C} \cap \{x_1 = 0.5\}$ translated by $(-0.1, 0)$. In this case the optimal trajectory necessarily crosses the collinearity and singular loci, see Fig.14 (right). While

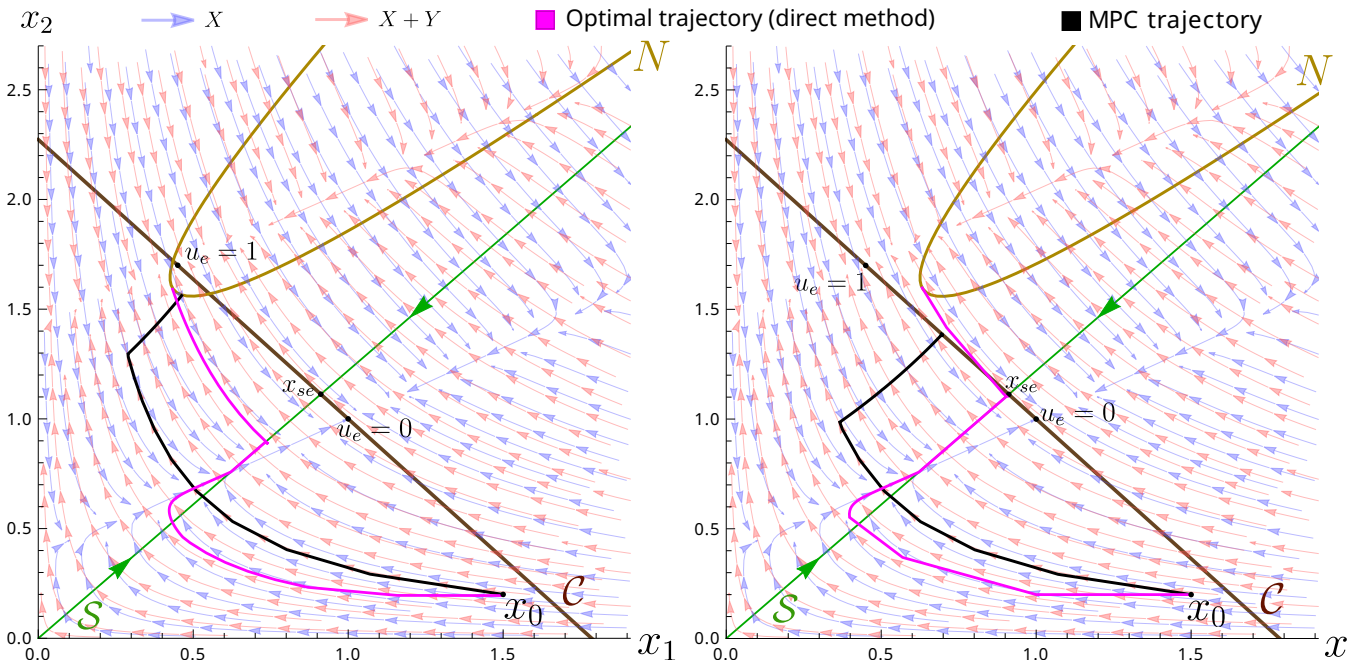

FIGURE 14 Geometric picture corresponding to Example b (a) (left) and Example b (b) (right) together with the trajectories obtained from the direct and MPC methods.

the policy from the direct method has again the bang–bang–singular–bang structure, the MPC method with $t_h = 1$, $h = 4$ does not reach $\boldsymbol{N}$ and terminates on the collinearity locus $\mathcal{C}$. This is expected since the horizon h of the MPC method is intricately related to the local controllability of the system. Below $\mathcal{C}$, the system can move in the direction of positive x_1 (since X points in this direction and $\det(X, Y) > 0$), while on $\mathcal{C}$ we need global policy to reach $\boldsymbol{N}$, that is a larger horizon has to be chosen otherwise the system stays on a forced equilibrium.

4.3.2 | Three dimensional case and the May and Leonard model

Uncontrolled dynamics

We begin by recalling the qualitative properties of the May and Leonard example (see also [22] and Appendix B):

$$\dot{x} = \operatorname{diag} x\,(\mathbf{1} - Ax), \tag{20}$$

where $x = (x_1, x_2, x_3)^\intercal$, $\mathbf{1} = (1, 1, 1)^\intercal$ and $A = \begin{pmatrix} 1 & \alpha & \beta \\ \beta & 1 & \alpha \\ \alpha & \beta & 1 \end{pmatrix}$, $\alpha > 0$, $\beta > 0$.

Contrary to the two dimensional case where the Poincaré-Bendixon applies, the analysis of the long term dynamics for three dimensional systems is intricate. Yet, one striking properties is the existence of a unique two dimensional Lipschitz manifold, called *carrying simplex*, containing all limit sets of (20) in the competitive case.

In the case where $\alpha + \beta > 2$ and $\alpha < 1$, the interior equilibrium $x_{es} = \kappa\,\mathbf{1}$, $\kappa = 1/(1 + \alpha + \beta)$ is unstable and the trajectories are getting closer and closer the three lines $\{x_1 + x_2 + x_3 = 1\} \cap \{x_i = 0\}$, $i = 1, 2, 3$, see Fig.15. Biologically speaking this means that a limit cycle among the three species can be produced.

Stratification of the terminal manifold

The plane $\mathcal{T} : x + y + z = 3\kappa$ is the tangent plane of the carrying simplex at x_{es}. Write

$$P = \begin{pmatrix} 1 & -1 & 1 \\ 0 & 2 & 1 \\ -1 & -1 & 1 \end{pmatrix}$$

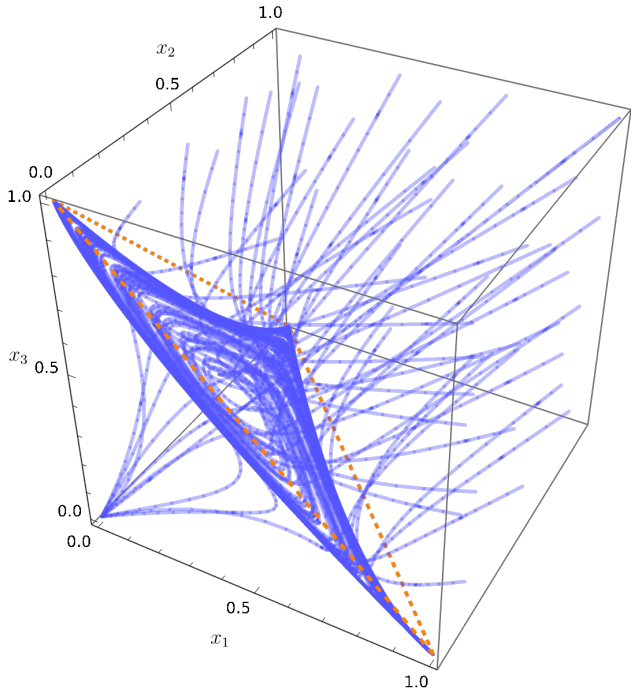

FIGURE 15 Trajectories of the May and Leonard system (20) which become recurrently closer to the orange dashed triangle.

and consider the boundary $\boldsymbol{N} = 0$ of the healthy region as the paraboloid with vertex x_{es} and such as $\mathcal{T}$ is the tangent plane of $\boldsymbol{N}$ at x_{es}. More precisely, the equation of $\boldsymbol{N}$ is $g(\boldsymbol{P}(x - x_{es})) = 0$, where g is the paraboloïd : $g(x) := x_3 - x_2^2 - x_1^2$.

Our objective here is to determine the local optimal policy to reach $\boldsymbol{N}$ in minimum time.

An extremal $z(.) = (x(.), p(.))$ arriving at time $t = 0$ at $x(0) \in \boldsymbol{N}$ is associated to the adjoint vector $p(0) = \nabla g(\boldsymbol{P}(x - x_{es}))_{|x=x(0)}$. We consider the case $x_{es} \in \Sigma_1 \cap \Sigma_2$, fulfilled when $\varepsilon_1 = -\varepsilon_2 - \varepsilon_3$ and this forces $x_{es} \in \mathcal{E}_0 \cap \mathcal{E}_1$, where $\Sigma_1, \Sigma_2, \mathcal{E}_0, \mathcal{E}_1$ are the strata:

$$
\begin{aligned}
\mathcal{E}_0 &:= \boldsymbol{N} \cap \{p(0) \cdot F(x) = 0\} \\
&= \boldsymbol{N} \cap \left\{3s^2\left(\alpha^2 + \alpha(2\beta - 3) + (\beta - 3)\beta - 1\right) + w^2\left(\alpha^2 + \alpha(2\beta - 7) + (\beta - 7)\beta + 1\right) + 6sw(\alpha - \beta) + o(|(w, s)|^2) = 0\right\} \\
\mathcal{E}_1 &:= \boldsymbol{N} \cap \{p(0) \cdot (F(x) + G(x)) = 0\} \\
&= \boldsymbol{N} \cap \left\{\varepsilon_2(3s(\alpha + \beta) - w(\alpha + \beta - 2)) - 2\varepsilon_3 w(\alpha + \beta - 2) + o(|(w, s)|) = 0\right\} \\
\Sigma_1 &:= \boldsymbol{N} \cap \{p(0) \cdot G(x) = 0\} \\
&= \boldsymbol{N} \cap \left\{\varepsilon_2\left(s\left(\frac{\alpha + \beta}{\alpha + \beta + 1} - \frac{1}{3}w(3w + 4)\right) + w\left(\frac{1}{\alpha + \beta + 1} + w^2 + w - \frac{1}{3}\right) - s^3 + s^2(w - 1)\right)\right. \\
&\qquad \left. + \frac{2}{3}\varepsilon_3 w\left(\frac{3}{\alpha + \beta + 1} + s(3s - 4) + 3w^2 - 1\right) = 0\right\} \\
\Sigma_2 &:= \boldsymbol{N} \cap \{p(0) \cdot [G, F](x) = 0\} \\
&= \boldsymbol{N} \cap \left\{\varepsilon_2\left(w\left(\alpha^2 - \alpha(\beta + 7) - \beta(2\beta + 1)\right) + 3s(\alpha(\alpha + \beta + 3) + 3\beta + 1) + w\right)\right. \\
&\qquad \left. + \varepsilon_3((\alpha + \beta)(3s(\alpha - \beta) - w(\alpha + \beta + 8)) + 2w) + o(|(w, s)|^2) = 0\right\}
\end{aligned}
$$

and x_{es} is an isolated point in $\mathcal{E}_0$. Moreover, since $p(0) \cdot G(x_{es}) = p(0) \cdot [G, F](x_{es}) = p(0) \cdot [[G, F], F](x_{es}) = 0$ and $p(0) \cdot [[G, F], G](x_{es}) = 2\left(\varepsilon_2^2 + \varepsilon_3\varepsilon_2 + \varepsilon_3^2\right)/(\alpha + \beta + 1) > 0$, x_{es} is a singular point of the singular dynamics.

For $x(0) \in \boldsymbol{N} \setminus \Sigma_1$, a simple rule to determine the bang control $u(0) \in \{0, 1\}$ reaching $\boldsymbol{N}$ is given by the relative position of F and $F + G$ with respect to $\boldsymbol{N}$:

(i) if $p(0) \cdot F(x(0))$ and $p(0) \cdot (F + G)(x(0))$ have the same sign then $u(0) = (1 + \operatorname{sign} p(0) \cdot G(x(0)))/2$ (see Fig. 17 *(right)*),

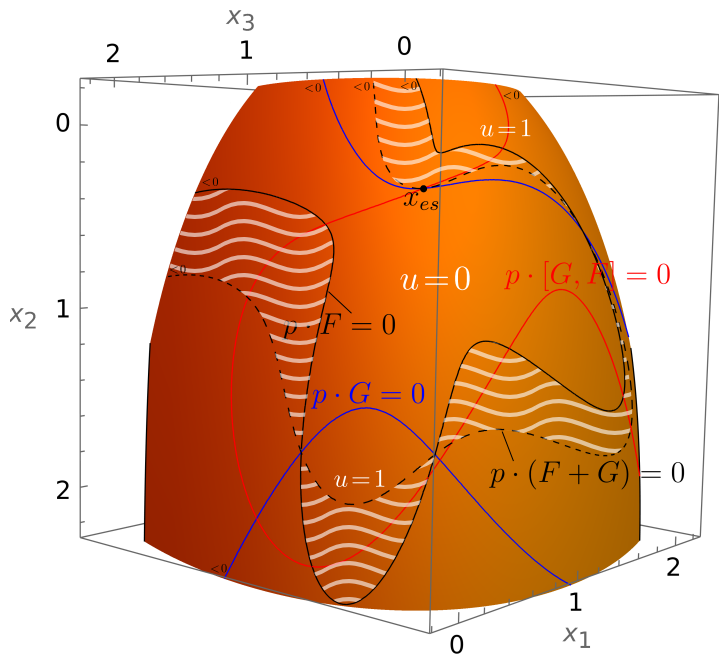

FIGURE 16 Stratification of the terminal manifold $\boldsymbol{N}$. The wavy white region corresponds to the case where $p(0)\cdot F(x(0))$ and $p(0)\cdot(F+G)(x(0))$ have opposite signs. In the other region the value of the control reaching a point $x(0)\in \boldsymbol{N}\setminus\Sigma_1$ is $u(0)=(1+\operatorname{sign} p(0)\cdot G(x(0)))/2$.

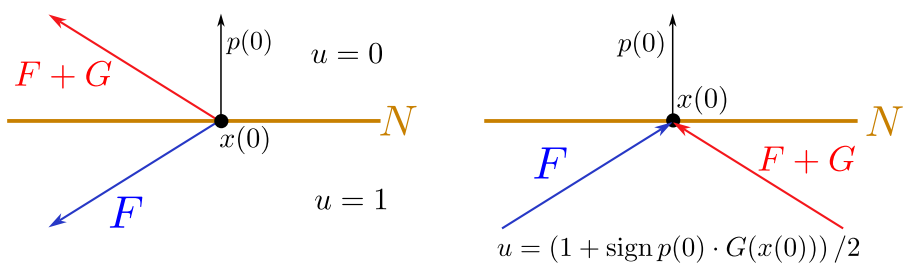

FIGURE 17 Control policy at an ordinary point. *(left)* Case (i). *(right)* Case (ii).

(ii) if $p(0)\cdot F(x(0))$ and $p(0)\cdot(F+G)(x(0))$ have opposite signs then there is only one $u\in\{0,1\}$ that reaches $\boldsymbol{N}$ (see Fig. 17 *(left)*).

The situation $x(0)\in\Sigma_1\setminus\Sigma_2$ may occur and in this case, the transversality condition yields $u(0)=(1+\operatorname{sign} p(0)\cdot[G,F](x(0)))/2$. Figure 16 summarizes the stratification and details the time minimal control reaching $\boldsymbol{N}$ for the parameters $\alpha=0.5$, $\beta=2$, $\varepsilon_1=0$, $\varepsilon_2=-1$.

For higher codimensional cases the local time optimal policy can also be determined using the dictionary of syntheses presented in Section 3.4 and the method described in [17]. In our example, the case $x(0)=x_{es}$ highlights such higher codimensional case and was analyzed in [7].

Direct and Model predictive control methods

The previous paragraph was devoted to determine local optimal policies – near the terminal surface $\boldsymbol{N}$. To compute global time optimal policies, we run both direct and MPC methods for the May and Leonard model with the following parameters : $\alpha=0.5$, $\beta=2$, $\varepsilon_1=0$, $\varepsilon_2=-1$, $\varepsilon_3=1$, $x_0=(0.2,0.25,0.35)$ and the terminal surface is the paraboloïd $\boldsymbol{N}$ introduced in the previous paragraph.

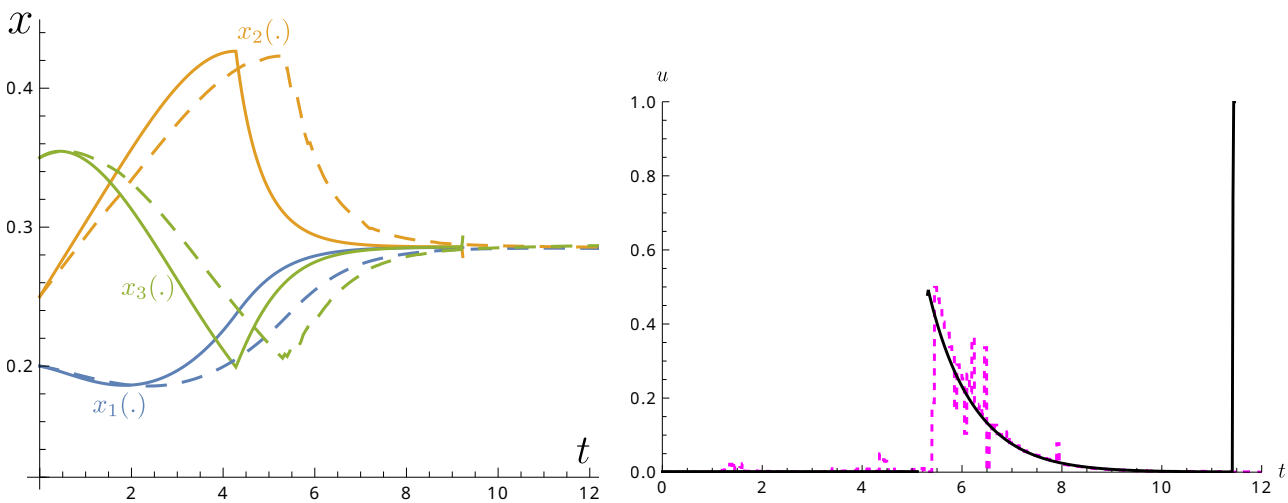

FIGURE 18 Time evolution of the states trajectories (left) and controls (right) for both direct (continuous lines) and MPC (dashed lines) methods reaching in minimum time the paraboloïd $\boldsymbol{N}$ for the May and Leonard system. The direct solution has bang-singular-bang structure while the MPC policy is "bang-singular".

The direct methods exhibits a $\sigma_-\sigma_s\sigma_+$ structure for the computed trajectory defined on $[0, 11.46]$. The MPC method computes a trajectory defined on $[0, 12.05]$, which behaves like a $\sigma_+\sigma_s$ arc, see Figure 18. Parameters used for this simulations are: $h = 3$, $t_h = 0.75$, $\delta = 0.05$ (outer time step) and $\eta = 10^{-8}$ (stopping criterion).

CONCLUSION

In this article we have presented mainly the techniques from geometric control theory to analyze reduction of the infection of a gut microbiote by a pathogenic agent using a controlled Lotka–Volterra model in dimension $N = 11$, which can admit up to $2^{11} = 2048$ interacting equilibria.

In the optimal control context the problem can be analyzed combining indirect or direct schemes in the permanent or sampled–data control frame both aspects are complementary. They were applied to the $2d$–case but can be generalized to the N–dimensional case, the limit being the computational complexity.

The problem illustrates the role of two feedback invariants, which are the collinearity and the singular loci to determine the optimal solution.

In the $2d$–case, each locus is a straight-line but in higher dimension the problem boils down to analyze the singular locus, which is foliated by singular trajectories and captures the nonlinearity of the model in the optimal control frame. Such a study has to be made in parallel with the geometry of the free dynamics introduced by Lotka–Volterra to model different interactions of the species defining cooperative or non cooperative interactions.

Hence a challenge in the control problem is to extend the study from the $2d$ to the $3d$ case. This leads to classify the singular dynamics and compute optimal solutions, combining geometric study with direct and indirect numerical methods. In this context the innovation of this article is to set the Lie algebraic frame in relation with robustness of the computations with respect to model uncertainties. A first step in this direction are the preliminary computations in the May–Leonard model.

In this article we restrict mainly to a single antibiotic or probiotic treatment. However the sampled-data control frame allows to treat a medical protocol combining different treatments with a dynamics described by:

$$\frac{\mathrm{d}x}{\mathrm{d}t} = X(x(t)) + \sum_{\substack{\text{antibiotic,}\\ \text{probiotic}}} u_i(t)\, Y_i(x(t)) + \sum_{\substack{\text{transplantation,}\\ \text{bactericide}}} u_i'(t)\, Y_i'(x(t)).$$

Additionally, it leads to compute the control as a closed loop control.

How to cite this article: B. Bonnard, J. Rouot, C. Silva, (2022), Geometric Optimal Control of the generalized Lotka-Volterra model of the Intestinal Microbiome, *Optimal Control Applications and Methods*, *2022*.

APPENDIX

A A RECAP OF ACCESSIBILITY RESULTS COMING FROM GEOMETRIC CONTROL

Definition 9. We shall denote by M a C^ω-manifold of dimension N connected and second countable which can be identified to $\mathbb{R}^N$ and $V(M)$ is the set of C^ω-vector field on M. If $F, G \in V(M)$, the *Lie bracket* is computed with the convention

$$[F, G](x) = \frac{\partial F}{\partial x}(x)G(x) - \frac{\partial G}{\partial x}(x)F(x).$$

If $F \in V(M)$, we denote by $x(t, x_0)$ the maximal solution on J of the Cauchy problem: $\frac{\mathrm{d}x}{\mathrm{d}t} = F(x)$, $x(0) = x_0$. We denote by $\{\exp tF\,;\, t \in J\}$ the (pseudo) one parameter group defined by $(\exp tF)(x_0) = x(t, x_0)$. Consider a control system of the form $\dfrac{\mathrm{d}x}{\mathrm{d}t} = F(x, u)$, where $u \in \mathcal{U}$ and $\mathcal{U}$ denotes the set of admissible controls which consists into the set of measurable mappings valued in the fixed control domain U. Taking $u \in L^\infty[0, T]$, the fixed time *extremity mapping* is the map

$$E^{x_0,T} \;:\; u \in \mathcal{U} \mapsto x(T, x_0, u),$$

where we assume that the response is defined on the whole $[0, T]$ and the extremity mapping is the map

$$E^{x_0} \;:\; u \in \mathcal{U} \mapsto x(\cdot, x_0, u).$$

In our accessibility study we can restrict to the set of piecewise constant mappings valued in U. Hence this leads to introduce the *polysystem* $D = \{F(x, u)\,;\, u \in U\}$. We denote by $S(D)$ the pseudo-semigroup generated by $\{\exp tF\,;\, F \in D, t > 0\}$ and $G(D)$ the pseudogroup generated by $S(D)$.

Taking x_0, x_1 we say that x_1 is *accessible* to x_0 in time T if there exists $t_1, \dots, t_k > 0$ such that $x_1 = \varphi\left(t_1, \dots, t_k\right) = \left(\exp t_k F_k \circ \dots \circ \exp t_1 F_1\right)(x_0)$, $t_i > 0$, $t_1 + t_2 + \dots + t_k = T$ and x_1 is *normally accessible* to x_0 in time T if additionally φ is a submersion. We denote by $A^+(x_0, T)$ the set of accessible points in time T and $A^+(x_0) = \cup_{T>0} A^+(x_0, T)$ the accessibility set. Reversing time, one can define similarly the sets $A^-(x_0, T)$, $A^-(x_0)$ of points which can be steered to x_0. The polysystem D is *controllable* in time T if for each x_0, $A^+(x_0, T) = M$ and controllable if, for each x_0, $A^+(x_0) = M$.

One has the following lemma.

Lemma 2. $A^+(x_0) = S(D)(x_0)$ (orbits of the pseudo-semigroup $S(D)$) and the system is controllable if $S(D)$ acts transitively on M.

Definition 10. The polysystem D is called weakly controllable if for each x_0, $G(D)(x_0) = M$.

This leads to the Chow-Rashevskii theorem that we formulate next.

Proposition 10. Let $F, G \in V(M)$ and $\varphi \in \mathrm{diff}(M)$. Denote $\varphi * F$ the image of F defined by $\varphi * F := \mathrm{d}\varphi\left(F \circ \varphi^{-1}\right)$. We have:

1. The one parameter pseudo-group of $G = \varphi * F$ is given by
$$\exp tG = \varphi \circ \exp tF \circ \varphi^{-1}.$$
2. $\varphi * [F, G] = [\varphi * F, \varphi * G]$.
3. The Baker-Campbell-Hausdorff formula is:
$$\exp sF \circ \exp tG = \exp \xi(F, G)$$
where $\xi(F, G)$ belongs to the Lie algebra generated by $\{F, G\}$ with:
$$\xi(F, G) = sF + tG + \frac{s\,t}{2}[F, G] + \frac{s\,t^2}{12}[[F, G], G] - \frac{s^2\,t}{12}[[F, G], F] - \frac{s^2 t^2}{24}[F, [G, [F, G]]] + \dots,$$
the series being converging for s, t small enough.

4. Denote by $\mathrm{ad}\, F \cdot G = [F, G]$ and $\varphi_t = \exp tF$ we have the $\mathtt{ad}$-formulae

$$\varphi_t * G = \sum_{k \geq 0} \frac{t^k}{k!} \mathtt{ad}^k F(G)$$

and the series is converging for t small enough.

Given two vector fields, an important computational problem is introduced next.

Definition 11. Let $D = \{F\}$ be a polysystem. We denote by $D_{L.A.}$ the Lie algebra generated by D computed recursively using iterated Lie brackets:

$$D_1 = \mathrm{span}\, D\,, \quad D_2 = \mathrm{span}\,\{D_1 + [D_1, D_1]\}\ \dots\,, D_k = \mathrm{span}\{D_{k-1} + \left[D_1, D_{k-1}\right]\}\,,$$

and

$$D_{L.A.} = \cup_{k \geq 1} D_k\,.$$

If $x \in M$, we introduce the following sequences of integers: $n_k(x) = \dim\, D_k(x)$. Let the derived Lie algebra given by $\left[D_{L.A.}, D_{L.A.}\right]$ and denote $D^0_{L.A.}$ the Lie algebra:

$$\left\{ \sum_{i=1}^{p} \lambda_i F^i + G\,;\, p \in \mathbb{N}\,, \lambda_i \in \mathbb{R}\,, \sum_{i=1}^{p} \lambda_i = 0\,, F^i \in D\,, G \in \left[D_{L.A.}, D_{L.A.}\right] \right\}\,.$$

Definition 12. Given two vectors fields F, G, a Hall basis is a minimal set of generators of the free Lie algebra generated by F and G. Let $x \in M$, a frame of minimal lengths is a set of iterated Lie brackets with full rank equals to $\dim M$ at x and where the sum of length of the iterated generators is minimal.

In particular, the following results are useful in our computations.

Lemma 3. Denote in short by $F\,G$ the Lie bracket $[F, G]$. If $D = \{F, G\}$ every Lie bracket of lengths smaller than 5 can be computed with the following 14 Lie products: $F, G, F\,G, F^2\,G, F\,G^2, F^3\,G, F^2\,G^2, F\,G^3, F^4\,G, F^3\,G^2, F^4\,G, F^3\,G^2, F^2\,G\,F\,G$, $F\,G\,F\,G^2$, $F^2\,G^3$, $F\,G^4$.

Application 1. Using log-coordinates one can compute, up to length 5, iterated Lie brackets of the polysystem

$$D = \{F,\, G\}$$

with $F = Ae^y + r$, $G = \left(\varepsilon_1, \dots, \varepsilon_N\right)^T$.

Theorem 2 (Chow-Rashevskii)**.** Let D be a C^ω-polysystem on M. Assume that for each $x \in M$, $\dim\, D_{L.A.}(x) = \dim\, M$. Then we have, for each $x \in M$:

$$G(D)(x) = G\left(D_{L.A.}(x)\right) = M\,.$$

Proof. The semi-constructive proof is to use Baker-Campbell-Hausdorff formula to construct a frame of iterated Lie brackets $F_1, \dots, F_n$ such that $\varphi\left(t_1, \dots, t_n\right) = \left(\exp t_1 F_1\right) \circ \dots \left(\exp t_n F_n\right)(x)$ is a local diffeomorphism at 0. □

In particular, this gives controllability result for a *symmetric polysystem* D, that is if $F \in D$, $-F \in D$. But the following weaker result is true [25] and we present Krener's proof.

Proposition 11. Let D be a polysystem such that $\dim D_{L.A.}(x) = \dim\, M$ for each $x \in M$. Then for every neighborhood V of x, there exists a non empty open set U contained in $V \cap A^+(x)$ (or $A^-(x)$).

Proof. Let $x \in M$, if $\dim M \geq 1$, then there exists $F_1 \in D$ such that $F_1(x) \neq 0$. Consider the integral curve

$$\alpha_1\ :\ t \mapsto \left(\exp\, t\, F_1\right)(x)\,.$$

If $\dim\, M \geq 2$, then there exists in every neighborhood V of x, a point $y \in M$ such that $y = \exp t_1 F_1$, $t_1 > 0$, and a vector field $F_2 \in D$ such that F_1 and F_2 are not collinear at y. Consider the mapping

$$\alpha_2\ :\ \left(t_1, t_2\right) \mapsto \left(\exp\, t_2 F_2\right) \circ \left(\exp\, t_1 F_1\right)(x)\,.$$

If $\dim\, M \geq 3$, one can iterate the construction at a point of the image for t_1, $t_2 > 0$. □

In Chow-Rashevskii's theorem, the semi-group action is extended to the group action, which amounts to use *non-feasible* controls for each leg $\exp t_i F_i$ if $t_i < 0$, $i = 1, \dots, N$. But a simple approach to obtain controllability is to replace each of such leg joining x to y by a leg of the form $\exp t'_i F'_i$, with $t'_i > 0$.
This leads to the following.

Definition 13. Let $F \in V(M)$. The point $x_0 \in M$ is said *Poisson stable* if for every $T > 0$ and every neighborhood V of x_0 there exist t_1, $t_2 \geq T$ such that $\exp t_1 F(x_0) \in V$ and $\exp -t_2 F(x_0) \in V$. The vector field F is called *Poisson stable* if the set of *Poisson stable* points is dense in M.

Proposition 12. Let D be a polysystem and assume the following:

1. for every $x \in M$, *rank* $D_{L.A.}(x) = \dim\ M$;
2. every vector field $F \in D$ is Poisson stable.

Then the system is controllable.

Outline of the proof. See [20] for the details. Taking $x, y \in M$, using Chow-Rashevskii's theorem one can write:

$$y = \exp\ t_k F_k \circ \dots \circ \exp\ t_1 F_1(x),$$

where $t_1, \dots, t_k$ are positive or negative.
In the previous sequence, each element of the form $\exp\ sF$ with $s < 0$ can be nearby replaced by an arc $\exp\ s'F,\ s' > 0$ using the Poisson stability property of F. The proof follows using Proposition 11. □

Next we present another approach to the accessibility problem [13], which can be applied to polynomic systems due to the work of [15].

Definition 14. Let D, D' be polysystems satisfying the *rank* condition $\dim\ D_{L.A.}(x) = \dim\ D'_{L.A.}(x) = \dim\ M\ , \forall x$. They are called *equivalent* if, for every $x \in M$, $\overline{S(D)(x)} = \overline{S(D')(x)}$. The union of all polysystems D' equivalent to D is called the *saturated* of D and is denoted by sat D.

Next, we present the set of operations to compute the *saturated* of D.

Proposition 13. Let D be a polysystem. Then:

1. If F, $G \in D$, then the convex cone generated by F and G belongs to *sat* D;
2. Let $F \in D$ and assume that F is Poisson stable, then $-F \in$ sat D;
3. If $\pm F$, $\pm G \in D$, then $\pm [F, G] \in$ sat D;
4. The *normalizer* $N(D)$ is the set of diffeomorphisms φ on M such that, for every $x \in M$, $\varphi(x)$ and $\varphi^{-1}(x)$ belongs to $\overline{S(D)(x)}$. One has:
   (a) If $\varphi \in N(D)$ and $F \in D$ then $\varphi * F \in$ sat D;
   (b) If $\pm F \in D$ and $G \in D$ then for $\varphi_\lambda = \exp\ \lambda\ F \in$ sat D, we have $\varphi_\lambda * G \in$ sat D, for every λ.

Remark 3. Remarks on the properties of Proposition 13:

- Property 2. comes from Proposition 12;
- Property 3. is a reformulation of Theorem 2;
- the concept of normalizer introduced in Property 4. is an important tool in the construction of sat D, in particular in relation with the ad-formula of Proposition 10.

Application 2. Accessibility properties of the pair $D = \{F, G\}$, $F = Ae^y + r$, $G = \left(\varepsilon_1, \dots, \varepsilon_N\right)^T$ can be analyzed using the previous techniques in relation with the analysis of the controlled GLV-equation. Nevertheless, a negative controllability result is the following.

Proposition 14. Consider on $\mathbb{R}^2\backslash\{0\}$ the pair of linear vectors fields $\{A_1x, A_2x\}$ and assume that A_1, A_2 are hyperbolic, that is, $A_i \sim \begin{pmatrix} \lambda_1 & 0 \\ 0 & \lambda_2 \end{pmatrix}$, $\lambda_1\lambda_2 < 0$. Then accessibility can be characterized by the intertwining of the stable and unstable directions.

Proof. Let $a > 0$ and $a' < 0$ denote the eigenvalues of A and $b > 0$ and $b' < 0$ the eigenvalues of B. Clearly $\dim\{Ax, Bx\}_{L.A.} = \mathbb{R}^2 \setminus \{0\}$ if and only if A and B have no common eigenvalues.

Let M_1 denote one intersection of the eigenspace of a with the unit circle and, using the positive orientation starting from M_1, denote M_2, M_3, M_4 the first intersection with the unit circle of the eigenspaces associated respectively to a', b and b'. Then the only controllable polysystems $\{Ax, Bx\}$ on $\mathbb{R}^2 \setminus \{0\}$ are associated to (M_1, M_2, M_3, M_4) or (M_1, M_4, M_3, M_2). This is clear since controllable pairs are such that for every $x \in \mathbb{R}^2 \setminus \{0\}$ there exists a periodic path surrounding 0 of the form: $\exp t_1X_1 \circ \ldots \circ \exp t_kX_k(x)$, with $t_i > 0$ and X_i in the polysystem $\{Ax, Bx\}$. □

Corollary 2. Let the polysystem $\{Ax, Bx + b\}$, where A and B are hyperbolic and b is non zero. Then it is controllable on $\mathbb{R}^2$ if $\{Ax, Bx\}$ is controllable on $\mathbb{R}^2 \setminus \{0\}$.

B COMPETITIVE LOTKA VOLTERRA SYSTEMS

In this appendix we use the reference [2].

Definition 15. A competitive Lotka-Volterra system between n-species is given by

$$\frac{\mathrm{d}x_i}{dt} = x_i(r_i - \sum_{j=1,\ldots,n} a_{ij}x_j),$$

where $a_{ij} > 0$, $r_i > 0$. We restrict the solutions to the non-negative cone $C = \mathbb{R}^n_+$. The origin O is a repeller.

A special case of interest is the assymetric May-Leonard system which takes the form

$$\frac{\mathrm{d}x_1}{dt} = x_1(1 - x_1 - a_{12}x_2 - a_{13}x_3),$$

$$\frac{\mathrm{d}x_2}{dt} = x_2(1 - x_2 - a_{21}x_1 - a_{23}x_3),$$

$$\frac{\mathrm{d}x_3}{dt} = x_3(1 - x_3 - a_{31}x_1 - a_{32}x_2)$$

The cone C contains an unique two-dimensional, compact invariant Lipschitz manifold called the carrying simplex denoted Σ which corresponds to the boundary of the basin of repulsion of the origin and attract every orbits except the origin. More generally the dynamics in the carrying simplex can be studied. The interior equilibrium E can be normalized to $(1, 1, 1)$ taking the normalization $r = \sum_j a_{ij}$. See [10] for the details of the dynamics, in particular for the number of limit cycles in the carrying simplex, in relation with the 16th Hilbert problem.

C MODEL PARAMETERS

The following tables give the parameters for the CDI model presented in [24].

Genera (sorted by susceptibility)	Growth (ρ_i)	Susceptibilities (ε_i)
Barnesiella	0.36807	-3.2926
undefined genus of Lachnospiraceae	0.31023	-3.0354
unclassified Lachnospiraceae	0.3561	-2.0909
Other	0.54006	-1.9395
Blautia	0.70898	-1.3491
undefined genus of unclassified Mollicutes	0.47064	-1.1018
Akkermansia	0.2297	-0.92446
Coprobacillus	0.83005	-0.79401
Clostridium difficile	0.39181	-0.31272
Enterococcus	0.29075	1.0671
undefined genus of Enterobacteriaceae	0.32367	3.7009

	Bar.	Und. Lac.	Uncl. Lac.	Other	Bla.	Und. Mol.	Akk.	Cop.	Und. En.	Ent.	C. diff.
Bar.	-0.205	0.098	0.167	-0.164	-0.143	0.019	-0.515	-0.391	-0.268	0.008	0.346
Und. Lac.	0.062	-0.104	-0.043	-0.154	-0.187	0.027	-0.459	-0.413	-0.196	0.022	0.301
Uncl. Lac.	0.143	-0.192	-0.101	-0.139	-0.165	0.013	-0.504	-0.772	-0.206	-0.006	0.292
Other	0.224	0.138	0.000	-0.831	-0.223	0.220	-0.205	-1.009	-0.400	-0.039	0.666
Bla.	-0.180	-0.051	0.000	-0.054	-0.708	0.016	-0.507	0.553	0.106	0.224	0.157
Und. Mol.	-0.111	-0.037	-0.042	0.041	0.261	-0.422	-0.185	-0.432	-0.264	-0.061	0.164
Akk.	-0.126	-0.185	-0.122	0.380	0.400	-0.160	-1.212	1.389	-0.096	0.191	-0.379
Cop.	-0.071	0.000	0.080	-0.454	-0.503	0.169	-0.562	-4.350	-0.207	-0.223	0.443
Und. Ent.	-0.374	0.278	0.248	-0.168	0.084	0.033	-0.232	-0.395	-0.384	-0.038	0.314
Ent.	-0.042	-0.013	0.024	-0.117	-0.328	0.020	0.054	-2.096	0.023	-0.192	0.111
C. diff.	-0.037	-0.033	-0.049	-0.090	-0.102	0.032	-0.181	-0.303	-0.007	0.014	-0.055

TABLE C1 *(top)* Growth rates ρ_i and susceptibilities ε_i of each microbial population i of the CDI model. *(bottom)* Interactions between pairwise microbial populations of the CDI model. These values are excerpted from the supplementary material of [24].

References

[1] M.T. Angulo, C.H. Moog, Y.Y. Liu, *A theoretical framework for controlling complex microbial communities*, Nature communications, **10** no.1045, (2019).

[2] S. Baigent, *Geometry of carrying simplices of 3-species competitive Lotka-Volterra systems*, Nonlinearity, **26**, (2013) 1001–1029.

[3] T. Bakir, B. Bonnard, L. Bourdin, J. Rouot, *Pontryagin-Type Conditions for Optimal Muscular Force Response to Functional Electrical Stimulations*, J. Optim. Theory Appl., **184**, (2020), 581–602.

[4] B. Bonnard, M. Chyba, *The role of singular trajectories in control theory*, Springer Verlag, New York, (2003), 357 pages.

[5] B. Bonnard, G. Launay, M. Pelletier, *Classification générique de synthèses temps minimales avec cible de codimension un et applications*, Annales de l'I.H.P. Analyse non linéaire, **14** no. 1, (1997), 55–102.

[6] B. Bonnard, J. Rouot, *Optimal Control of the Controlled Lotka-Volterra Equations with Applications - The Permanent Case*, SIAM J. Appl. Dyn., **22**, no. 4, (2023), 2761–2791.

[7] B. Bonnard, J. Rouot, *Feedback Classification and Optimal Control with Applications to the Controlled Lotka–Volterra Model*, Preprint 2022, hal-03917363

[8] B. Bonnard, J. Rouot, B. Wembe, *Accessibility Properties of Abnormal Geodesics in Optimal Control Illustrated by Two Case Studies*, Math. Control Relat. Fields, **13** no. 4, (2023), 1618–1638.

[9] L. Bourdin, E. Trélat, *Optimal sampled-data control, and generalizations on time scales*, Math. Control Relat. Fields, **6** no. 1, (2016), 53–94.

[10] J. Hofbauer, J. W.-H. So, *Multiple limit cycles for three dimensional Lotka-Volterra equations*, Applied Math. Lett., **7**, no. 6, (1994) 65–70.

[11] A. Isidori, *Nonlinear Control Systems*, 3rd ed. Berlin, Germany: Springer-Verlag, 1995, 549 pages.

[12] E. W. Jones, P. Shankin-Clarke, J. M. Carlson, *Navigation and control of outcomes in a generalized Lotka-Volterra model of the microbiome*, in Advances in Nonlinear Biological Systems: Modeling and Optimal Control, AIMS Series on Applied Mathematics, **11**, (2020), 97–120 .

[13] V. Jurdjevic, *Geometric Control Theory*, Cambridge Studies in Advanced Mathematics, **52** Cambridge University Press, Cambridge, 1997, 492 pages.

[14] A. J. Krener, *The high order maximal principle and its application to singular extremals*, SIAM Journal on Control and Optimization, **15** no. 15, (1977), 256–293 .

[15] H. Kunita, *On the Controllability of Nonlinear Systems with Applications to Polynomial Systems*, Appl. Math. Optim., **5**, (1979), 89–99.

[16] I. Kupka, *Geometric theory of extremals in optimal control problems. I. The fold and Maxwell case*, Trans. Amer. Math. Soc., **299** no.1, (1987), 225–243.

[17] G. Launay, M. Pelletier, *The generic local structure of time-optimal synthesis with a target of codimension one in dimension greater than two*, Journal of Dynamical and Control Systems, **3** no.165, (1997), 165–203.

[18] S. Lefschetz, *Differential equations: geometric theory*, Dover New York, 1977, 390 pages.

[19] E. B. Lee and L. Markus, *Foundations of Optimal Control Theory*, John Wiley and Sons, Inc., New York, 1967, 576 pages.

[20] C. Lobry, *Controllability of nonlinear systems on compact manifolds*, SIAM J. Control, **12**, (1974), 1–4.

[21] A.J. Lotka, *Elements of mathematical biology*, Dover Publications, Inc., New York, 1958, 465 pages.

[22] R.M. May, W.J. Leonard, *Nonlinear aspects of competition between three species.* SIAM J. Appl. Math., **29** (1975), pp. 243–253.

[23] L.S. Pontryagin, V.G. Boltyanskii, R.V. Gamkrelidze, E.F. Mishchenko, *The mathematical theory of optimal processes*, Oxford, Pergamon Press, 1964, 362 pages.

[24] R. R. Stein, V. Bucci, N. C. Toussaint, C. G. Buffie, G. Rätsch, E. G. Pamer, et al., *Ecological Modeling from Time-Series Inference: Insight into Dynamics and Stability of Intestinal Microbiota*, PLoS Comput Biol, **9** no. 12, (2013).

[25] H. J. Sussmann, V. Jurdjevic, *Controllability of nonlinear systems*, Journal of Differential Equations, **12**, no. 1, (1972), 95–116.

[26] H. Sussmann, *Nonlinear Controllability and Optimal Control*, ed., Marcel Dekker, New York, 1990, 477 pages.

[27] V. Volterra, *Leçons sur la théorie mathématique de la lutte pour la vie*, Les Grands Classiques Gauthier-Villars. Éditions Jacques Gabay, Sceaux, 1990, 215 pages.

[28] Y. Wang, S. Boyd, *Fast model predictive control using online optimization*, IEEE Transactions on control systems technology, **18** no. 2, (2010), 267–278.

ACKNOWLEDGMENTS

The first two authors for this research article benefited from the support of the FMJH Program PGMO and from the support of EDF, Thales, Orange. Silva was supported by Portuguese funds through CIDMA, The Center for Research and Development in Mathematics and Applications of University of Aveiro, and the Portuguese Foundation for Science and Technology (FCT–Fundação para a Ciência e a Tecnologia), within project UIDB/04106/2020 and by the FCT Researcher Program CEEC Individual 2018 with reference CEECIND/00564/2018.

AUTHOR BIOGRAPHY

Bernard Bonnard. Ph.D. degree in Mathematics, 1978 University of Metz and Thèse d'État ès Sciences, 1983, INPG and University of Grenoble. Postdoctoral positions: Control Theory Center, University of Warwick and Division Applied Sciences Harvard University. Permanent CNRS researcher from 1979 to 1991. Professor University of Burgundy, Institut de Mathématiques de Bourgogne, since 1991 and INRIA Sophia Antipolis researcher since 2011 (McTAO Team). Author of four books in Optimal Control and more than 130 research articles in optimal control, dynamical systems and geometry with applications to space mechanics, quantum control, magnetic resonance imaging, biomedical models (microswimmers, generalized Lotka-Volterra equations and microbiote, Hill–Huxley model in biomechanics).

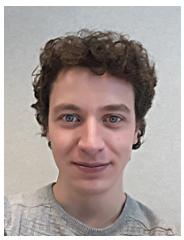

Jérémy Rouot. Ph.D. degree in Mathematics in 2016 from University Nice Côte d'Azur for its works in Optimal Control motivated by microswimming and space mechanics applications. In 2017, he worked as a postdoc in LAAS-CNRS (Toulouse) on the inverse optimal control problem. From 2017 to 2021, he was lecturer and researcher in two engineering schools EPF (Troyes) and ISEN (Brest) and since 2021, he is associate professor from the University of Western Brittany, LMBA (Brest) working on non smooth optimal control, optimal synthesis with applications to chemical reactors and mathematical biology.

Cristiana J. Silva. Cristiana J. Silva received her Ph.D. degree in Mathematics from the University of Orléans, in France, and from the University of Aveiro, in Portugal, in 2010. From 2011 to 2018, she was a post-doctoral researcher in Center for Research and Development in Mathematics and Applications (CIDMA) of the University of Aveiro and, between 2019 and 2022, she had a Researcher position at CIDMA. Since September 2022 she is Assistant Professor at Iscte - Instituto Universitário de Lisboa, in Lisbon, Portugal. Her research interests include optimal control theory, optimization methods and mathematical modeling of infectious diseases.